Knot theory and statistical mechanics

F. Y. Wu

Department of Physics, Northeastern University, Boston, Massachusetts 02115

This is a tutorial review on knot invariants and their construction using the method of statistical mechanics. We begin with brief reviews of the elements of knot theory and relevant results in statistical mechanics. We then show how knot invariants, including those discovered recently, can be obtained by applying techniques used in solving lattice models in lattice statistics. Our approach is based on the consideration of solvable models with strictly local Boltzmann weights. The presentation, which is self-contained and elementary, is intended for a general readership. A table of polynomial invariants for knot and links containing up to six crossings is included in the Appendix.

CONTENTS

I. INTRODUCTION

An exciting development occurring recently in the mathematical theory of knots and links is the discovery of new knot invariants (Freyd *et al.*, 1985; Jones, 1985; Akutsu and Wadati, 1987a; Kauffman, 1990) and their connection with statistical mechanics (Kauffman, 1987a; Jones, 1989). Particularly, the newly discovered connection with statistical mechanics has permitted a simple and direct formulation of knot invariants, a long-standing fundamental problem in knot theory. (For an account of these developments readable by nonexperts see Jones, 1990a).

Knots and links are loops of strings possessing threading and knotting properties that are topological in nature. To characterize these topological properties algebraically, mathematicians have found that certain polynomials can be used. These polynomials are knot invariants. Traditionally, each of the polynomial invariants was discovered and constructed under different circumstances, often requiring lengthy and tedious analyses. While knot invariants can now be analyzed using braid groups and understood within the framework of quantum groups (see, for example, Reshetikhin and Turaev, 1991), the statistical mechanical approach remains, in contrast, simple and elementary. Despite its simplicity and usefulness, however, the connection of knot invariants with sta-

Copyright ©1992 The American Physical Society

tistical mechanics has remained largely a topic unfamiliar to physicists, including many in the community of statistical mechanics where the main idea of the new approach is rooted. To be sure, a number of monographs and articles addressing the connection of knot theory with physics have appeared recently (e.g., Kauffman, 1988a, 1988b, 1991; Turaev, 1988; Jones, 1989; Wadati *et al.*, 1989; Yang and Ge, 1989), but they have been written mostly for mathematicians and cover aspects that may not be familiar to all physicists. There exists an apparent gap of communication between these two communities.

The purpose of this review is to introduce the recent advances in knot theory to physicists, explain what knot invariants are about, and show how they can be derived and understood from the point of view of statistical physics. To accomplish this, it is necessary to reformulate and rework a large body of existing and known results in knot theory and recast them within the framework of conventional statistical mechanics. The scope of this review is therefore necessarily limited, and confined only to the stated purpose. It is not our intent to review knot theory, nor do we intend to explore the braid group and the associated algebraic approach. We also do not discuss the role played by knot invariants in topological field theory (Witten, 1989a, 1989b, 1990), which could be the topic of a treatise by itself.

This review assumes no prior knowledge of knot theory and statistical mechanics and is therefore self-contained and suitable for a general readership. We shall cite and refer to original references as they arise in the course of our presentation, but no attempt will be made at a complete literature survey. Readers are referred to two recent books by Kohno (1991) and Kauffman (1991), which contain complete listings of the relevant literature in mathematics.

The organization of this review is as follows: In Sec. II we present elements of knot theory and introduce knot invariants and their traditional definition in terms of the Skein relation. The basic idea of approaching knot invariants using statistical mechanical methods is explained in Sec. III. This is followed by a review of relevant solvable, or integrable, vertex models in Sec. IV. These results are used in Sec. V to obtain knot invariants. We next show in Sec. VI that interaction-round-a-face (IRF) models can always be formulated as vertex models and use this formulation to derive knot invariants from IRF models. In Sec. VII we consider the construction of knot invariants from edge-interaction models, the spin models with pure two-spin interactions. For completeness we include in the Appendix a table of knot invariants for prime knots and links containing six or fewer crossings.

II. THEORY OF KNOTS

A. Definitions

We begin with a description of some terms in knot theory. A knot is the embedding of a circle, or a nonintersecting loop, in three-dimensional space. A link is a collection of two or more knots, or components, which may or may not be physically intertwined. In this paper we use the term *knot* loosely to denote either a single-component knot or a link. A knot is *oriented* if its loops are directed; otherwise, the knot is *unoriented.* While knots are unoriented to begin with, it is often convenient to direct the loops and consider oriented knots. Starting from a given unoriented knot consisting of n components, one has generally 2^n versions of oriented knots.

Knots can be projected onto a plane and thus represented by planar diagrams. We shall always have planar diagrams, or projections, in mind when we speak of knots. Diagrams of some simple knots are shown in Fig. 1. It can be seen that when using planar diagrams to represent knots we need to break one of the two lines crossing at an intersection to indicate their relative positionings in three-dimensional space. For oriented knots this leads to two kinds of line crossings, denoted by the signs + and −, as shown in Fig. 2, where the + and − crossings are related by a 90° rotation.

An intrinsic property, the *writhe* $w(K)$, of a knot K is defined by first orienting the knot and then computing

$$w(K)=n_+-n_- , \tag{2.1}$$

where n_+ and n_- are, respectively, the numbers of + and − crossings in the knot. For single-component knots the writhe $w(K)$ is uniquely defined, independent of the line orientation chosen. For example, the writhe of the right-handed trefoil in Fig. 1(c) remains 3 if the orientation is reversed. For knots with two or more components, the writhe will generally depend on the relative orientations of the components.

An *unknot* is a knot represented by a circle. Two knots are equivalent if they can be transformed into each other by a continuous deformation of the lines. Thus the knot in Fig. 1(b) is equivalent to an unknot and, in fact, all single-component knots with one or two crossings are equivalent to an unknot. The simplest nontrivial knot is the trefoil with three crossings. There are a total of 12 965 distinct single-component knots with 13 or fewer crossings, excluding mirror images, for which a complete

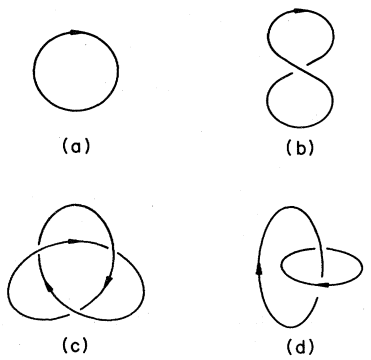

FIG. 1. Examples of planar representations of oriented knots: (a) and (b), unknot; (c) right-handed trefoil; (d) Hopf link.

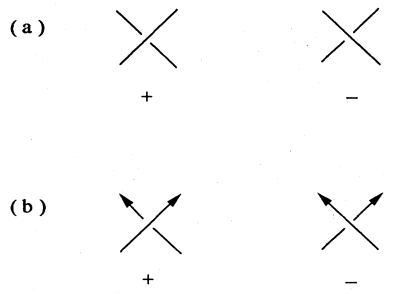

FIG. 2. Two kinds of line crossings: (a) unoriented knots, (b) oriented knots.

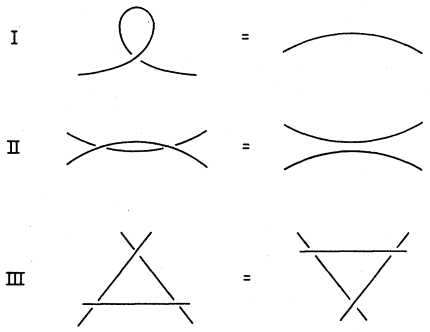

FIG. 3. Three types of Reidemeister moves for unoriented knots.

tabulation exists (Thistlethwaite, 1985).

While it is relatively easy to verify by inspection that the two knots in Figs. 1(a) and 1(b) are indeed equivalent, it is generally difficult to identify the equivalence of knots without doing some tedious checking. The problem lies in the fact that two equivalent knots may have very different planar projections. This leads to the need for characterizing knots algebraically. The idea is to associate algebraic functions with knots such that equivalent knots possess the same identical function. Such algebraic functions are the topological invariants of knots, or simply *knot invariants.* It should be mentioned that, despite recent progress, the construction of knot invariants that are different for all distinct knots still remains an open problem.

B. Reidemeister moves

As a first step in constructing knot invariants, one needs to understand the process of deforming knots. To this end it was shown by Reidemeister (1948) that all deformations of knots (in three-dimensional space) can be broken down into sequences of three basic types of line moves (in the two-dimensional projection), the Reidemeister moves. Thus it is sufficient to consider each of the three Reidemeister moves individually. We describe these moves for oriented and unoriented knots separately.

1. Unoriented knots

The three types of Reidemeister moves for unoriented knots are shown in Fig. 3; all other moves can be obtained from those shown by applying a rotation and/or a reflection. The algebraic function associated with a knot is said to be of an invariant of *ambient isotopy* if it is invariant under all I, II, and III types of moves, and of *regular isotopy* if invariant under the type-II and type-III moves only.

2. Oriented knots

The consideration of Reidemeister moves is more involved for oriented knots, since the lines are directed, thus breaking some symmetry. However, the basic topology of the moves remains unaltered. For type-I and type-II moves, it can be seen that there exists two independent moves of each type. These are the moves shown in Fig. 4; all other type-I and type-II moves can be obtained from those shown by applying a rotation and/or a reflection. For example, a reflection of the move IIA about a horizontal axis yields a move given by the same diagram but with the crossings + and − interchanged.

The type-III moves for oriented knots require more attention. Basically, there exist two distinct kinds of line orientations, types IIIA and IIIB, shown in Figs. 5 and 6, which differ in the way that the three lines are oriented. In each kind of line orientation, there further exist six distinct possible moves, and all other type-III moves are related to those shown by rotations and/or reflections. Note that the Reidemeister moves shown are those dictated by legitimate line moves (in three-dimensional

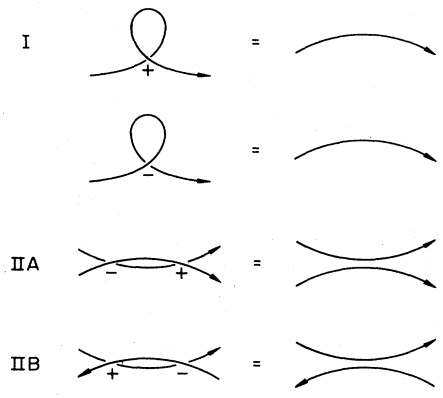

FIG. 4. Type-I and type-II Reidemeister moves for oriented knots. In move IIA the two lines point into the same half-plane, and in move IIB the lines point in opposite directions.

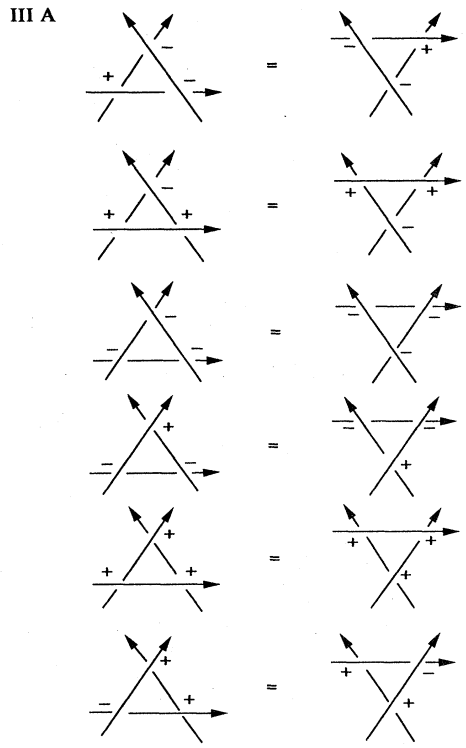

FIG. 5. Type-IIIA moves for oriented knots. The three lines are oriented to point into the same half-plane.

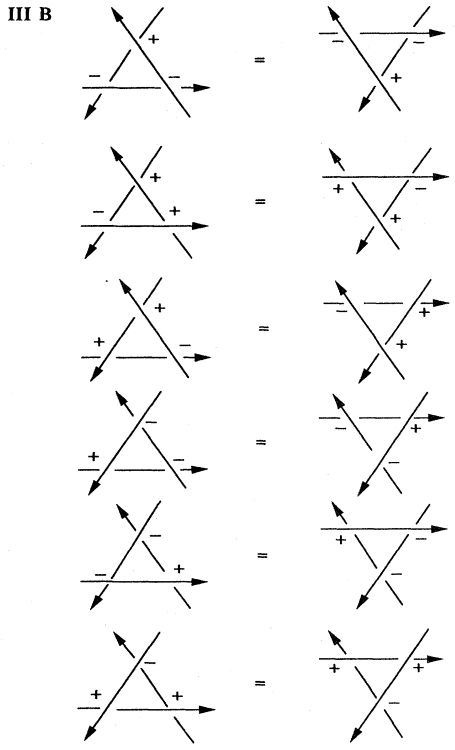

FIG. 6. Type-IIIB moves for oriented knots. The three lines are oriented to form a net circulation.

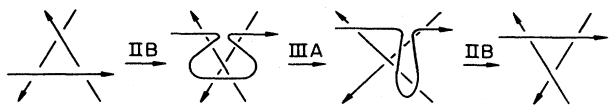

FIG. 7. A type-IIIB move as deduced from type-IIB and one of the six type-IIIA moves.

space), and therefore are not necessarily all independent. In fact, it suffices to consider only the type-I and type-II moves shown in Fig. 4 and any one of the six IIIA moves. All other moves, including the six-type-IIIB, follow as a consequence (Turaev, 1988). We include in Fig. 7 an example of how the type-IIIB move shown in the second line of Fig. 6 can be deduced by using the IIB and one of the IIIA moves (Kauffman, 1991). For comparison, we show in Fig. 8 configurations that cannot be disentangled by line moves. Note that configurations in Fig. 8 complement those in Figs. 4–6, so that altogether they give rise to all possible kinds of crossings that two and three lines can form.

As in the case of unoriented knots, the term ambient isotopy refers to invariance under all types (I, II, and III) of moves, and regular isotopy to invariance under type-II and type-III moves only. It is clear that the writhe $w(K)$ of a knot given by Eq. (2.1) is regular isotopy invariant, and that, under type-I moves, it changes by 1.

C. The Skein relation

Skein relations are recursion relations relating the invariants of knots whose diagrams are identical except that the connectivity of lines in a small region embedded in the knot is different. The most common Skein relations are described below.

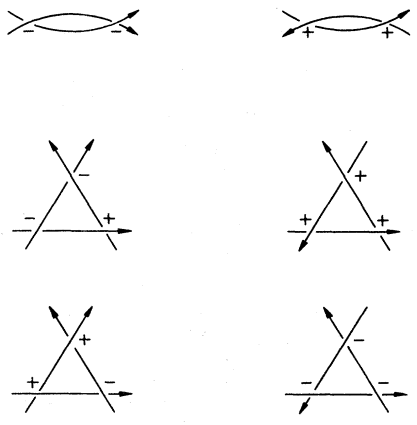

FIG. 8. Configurations that cannot be disentangled by line moves.

FIG. 9. The three line configurations considered in the Skein relation for oriented knots.

1. Oriented knots

For oriented knots there are two kinds of line crossings denoted by the signs + and − shown in Fig. 2 and again in Fig. 9. If a plus-type line crossing in a given knot is switched to a minus type, we arrive at, of course, a different knot. Furthermore, if the crossing is spliced so that it is replaced by a configuration denoted by 0 in Fig. 9, one obtains yet a third knot. We denote the three knots, respectively, by L_+, L_-, and L_0 and their associated invariants P_{L_+}, P_{L_-}, and P_{L_0}. The simplest Skein relation is then a recursion relation connecting these three P functions,

$$xP_{L_+}(x,y,z)+yP_{L_-}(x,y,z)=zP_{L_0}(x,y,z)\ , \tag{2.2}$$

where x, y, z are variables of the invariant.

The knot containing the configuration L_0 is simpler in the sense that it contains one less line crossing than the other two. Then, by applying the Skein relation Eq. (2.2) and Reidemeister moves repeatedly, one eventually equates the P function of any knot to a product of two factors: a Laurent polynomial of homogeneous degree zero in variables x, y, and z, and $P_{\text{unknot}}(x,y,z)$, the P function of an unknot which, without loss of generality, can be taken to be $P_{\text{unknot}}(x,y,z)=1$. Thus the P function is a Laurent polynomial of degree zero in x, y, z.

For example, applying Eq. (2.2) to the three knots shown in the first row in Fig. 10, one obtains

$$x\cdot 1+y\cdot 1=zP_{2l}(x,y,z)\ , \tag{2.2a}$$

and thus the P function for two unlinked loops is $P_{2l}(x,y,z)=(x+y)/z$. Applying the Skein relation to the three knots in the second row in Fig. 10, one obtains

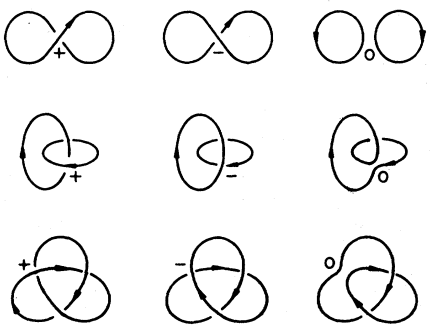

FIG. 10. Examples of knots connected by the Skein relation.

$$xP_{\text{Hopf}}(x,y,z)+y\cdot\frac{1}{z}(x+y)=z\cdot 1\ , \tag{2.2b}$$

and hence the P function for the Hopf link is $P_{\text{Hopf}}=(z^2-xy-y^2)/xz$. From the third row of Fig. 10 one has

$$xP_{\text{RT}}(x,y,z)+y\cdot 1=z\cdot\frac{1}{xz}(z^2-xy-y^2)\ , \tag{2.2c}$$

leading to the P function $P_{\text{RT}}(x,y,z)=(z^2-2xy-y^2)/x^2$ for the right-handed trefoil. One may also verify that the same results are always reached, independent of the order in which the Skein relation is applied to line crossings.

For the P function to be a true knot invariant, we need to ascertain its existence and uniqueness. That is, the P function so obtained is independent of the order in which the Skein relation is applied to line crossings for *arbitrary* knots. This is the crux of this approach. Indeed, the fact that the Skein relation Eq. (2.2) with general x, y, and z actually defines a knot invariant, the Homfly polynomial, was not recognized until very recently (Freyd *et al.* 1985), and only after its validity in two special instances became known (Conway, 1970; Jones, 1985).

The P function of the mirror image of a knot is obtained by interchanging x and y, since reflections interchange the crossings + and −. For example, the mirror image of the right-handed trefoil of Fig. 1(c) produces a left-handed trefoil with the invariant $P_{\text{LT}}(x,y,z)=(z^2-2xy-x^2)/y^2$. It is also clear that the reversal of all arrows does not change the ± types of crossings and therefore leaves the P function unchanged. But the reversal of arrows in one component of a link generally leads to a different P function.

2. Unoriented knots

Skein relations can be similarly written down for unoriented knots. However, as the four lines at a crossing can now be connected in four different ways, denoted by +, −, 0, and ∞, as shown in Fig. 11, the Skein relation for unoriented knots relates four functions P_{D_+}, P_{D_-}, P_{D_0}, and P_{D_∞}, where D_+ is the knot with the configuration +, etc. An example is the Skein relation for the Kauffman polynomial (Kauffman, 1990) given in Sec. II.D.5.

3. Other Skein relations

More generally, one can define Skein relations relating knots that differ in a small disk containing other types of

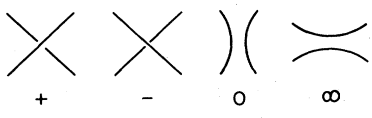

FIG. 11. The four line configurations considered in the Skein relation for unoriented knots.

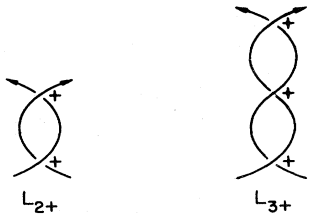

FIG. 12. Line configurations for the general Skein relation.

configurations, such as those denoted by L_{2+}, L_{3+} in Fig. 12. The Akutsu-Wadati polynomial satisfies Skein relations relating precisely these configurations.

D. Polynomial invariants

In this section we give the traditional definition of several known knot invariants using the Skein relation.

1. The Alexander-Conway polynomial

Alexander (1928) discovered the first knot invariant $\Delta(t)$ for oriented knots. His derivation is a combinatorial one. Years later Conway (1970) obtained an invariant $\nabla(z)$, the Conway polynomial, and showed that it can be determined from the Skein relation

$$\nabla_{L_+}(z)-\nabla_{L_-}(z)=z\nabla_{L_0}(z) \tag{2.3}$$

in conjunction with the conditions that $\nabla(z)$ be ambient isotopy invariant and

$$\nabla_{\text{unknot}}(z)=1 . \tag{2.4}$$

He further showed that $\nabla(z)$ is related to the Alexander polynomial $\Delta(t)$ through the relation

$$\nabla(z)=\Delta(t), \quad z=\frac{1}{\sqrt{t}}-\sqrt{t} . \tag{2.5}$$

It is clear that the Skein relation (2.3) is a special case of Eq. (2.2) with $x=1$, $y=-1$. Alexander polynomials of single-component knots are polynomials of z^2 (Lickorish and Millett, 1987) and are therefore symmetric in t and $1/t$. It also follows from Eq. (2.3) that the Alexander-Conway polynomial of a knot containing unlinked components vanishes identically. Until the discovery of the Jones polynomial in 1984, the Alexander-Conway polynomial had remained as the single known and useful polynomial invariant for decades.

2. The Jones polynomial

As alluded to earlier in Sec. I, recent advances in knot theory were brought about by Jones' discovery several years ago (Jones, 1985) of a new polynomial invariant $V(t)$, now known as the Jones polynomial. While Jones originally obtained $V(t)$ by analyzing the braid-group representation of knots using von Neumann algebras, he also pointed out that $V(t)$ satisfies the Skein relation[1]

$$\frac{1}{t}V_{L_+}(t)-tV_{L_-}(t)=\left[\sqrt{t}-\frac{1}{\sqrt{t}}\right]V_{L_0}(t) \tag{2.6}$$

and can be determined from it by further requiring ambient isotopy invariance and

$$V_{\text{unknot}}(t)=1 . \tag{2.7}$$

3. The Homfly polynomial

The similarity between the Jones and Alexander polynomials in terms of the Skein relation is very appealing. Within a few months after the announcement of Jones' result, four groups of researchers (Freyd *et al.*, 1985; see also Hoste, 1986; Lickorish and Millett, 1987) independently extended Jones's result to arrive at a new invariant. They showed that the Skein relation (2.2) with general x,y,z indeed defines a two-variable invariant, the Homfly polynomial.[2] This new invariant, which has since been rederived and analyzed by Jones (1987) using the Hecke algebra representation of the braid group, can be defined by rewriting the Skein relation (2.2) in the equivalent form

$$\frac{1}{t}P_{L_+}(t,z)-tP_{L_-}(t,z)=zP_{L_0}(t,z) . \tag{2.8}$$

The Homfly polynomial $P(t,z)$ is then completely determined from the Skein relation (2.8), the requirement of ambient isotopy, and the condition

$$P_{\text{unknot}}(t,z)=1 . \tag{2.9}$$

We have the relations

$$\nabla(z)=P(1,z), \quad V(t)=P(t,\sqrt{t}-1/\sqrt{t}) . \tag{2.10}$$

4. The Akutsu-Wadati polynomial

The Akutsu-Wadati polynomial is an example of a new knot invariant derived from exactly solvable models in statistical mechanics (Akutsu and Wadati, 1987a). For each $N=2,3,\ldots,$ the Akutsu-Wadati polynomial $A^{(N)}(t)$ is a Laurent polynomial in t satisfying ambient

[1]The definition of $V(t)$ adopted here is the same as that used in Jones (1987) and Kauffman (1991), and differs from that in Jones (1985) and Freyd *et al.* (1985) by the change of $t\to 1/t$.

[2]Named after the initials of the six coauthors of Freyd *et al.* (1985). A fifth group of researchers also obtained the same results. However, their announcement (Przytycki and Traczyk, 1987) arrived late due to slow mail (from Poland) and was not included in the joint paper.

isotopy invariance. For $N=2$ the Akutsu-Wadati polynomial coincides with the Jones polynomial, that is, we have

$$A^{(2)}(t)=V(t)\ , \tag{2.11}$$

which satisfies the Skein relation (2.6). For general N, however, the Akutsu-Wadati polynomial satisfies a Skein relation connecting knots differing in a small disk containing configurations L_0, L_-, and L_{n+}, with $n=1,2,\ldots,N-1$. For $N=3$, for example, the Skein relation is

$$A^{(3)}_{L_{2+}}(t)=t(1-t^2+t^3)A^{(3)}_{L_+}(t)+t^2(t^2-t^3+t^5)\times A^{(3)}_{L_0}(t)-t^8A^{(3)}_{L_-}(t)\ . \tag{2.12}$$

5. The Kauffman polynomial

The Kauffman polynomial (Kauffman, 1990) is a two-variable invariant of regular isotopy for unoriented knots. That is, it is invariant only under type-II and type-III Reidemeister moves. The Kauffman polynomial $L(\alpha,z)$ is defined by the Skein relation

$$L_{D_+}(\alpha,z)+L_{D_-}(\alpha z)=z[L_{D_0}(\alpha,z)+L_{D_\infty}(\alpha,z)]\ , \tag{2.13}$$

where $+$, $-$, 0, and ∞ are configurations shown in Fig. 11, and L_{D_+}, L_{D_-}, L_{D_0}, L_{D_∞} are the Kauffman polynomials of four knots D_+, D_-, D_0, D_∞ that are identical except that a small disk containing a single line crossing is replaced by the respective configurations $+$, $-$, 0, and ∞. In addition, the Kauffman polynomial is required to satisfy regular isotopy and the conditions

$$L_{\text{unknot}}(\alpha,z)=1\ , \tag{2.14}$$

$$L_{G_\pm}(\alpha,z)=\alpha^{\mp 1}L_{G_0}(\alpha,z)\ , \tag{2.15}$$

Here, G_0, G_+, G_- are configurations shown in Fig. 13, and $L_{G_0}(\alpha,z)$, $L_{G_+}(\alpha,z)$, and $L_{G_-}(\alpha,z)$ are the Kauffman polynomials of three knots that are identical except that one disk containing two incident lines is replaced by G_0, G_+, and G_-, respectively.

For our purposes it is convenient to consider the Dubrovnik version[3] of the Kauffman polynomial. The Dubrovnik version of the Kauffman polynomial, $Q(\alpha,z)$ is defined by the Skein relation

$$Q_{D_+}(\alpha,z)-Q_{D_-}(\alpha,z)=z[Q_{D_0}(\alpha,z)-Q_{D_\infty}(\alpha,z)] \tag{2.13a}$$

and subject to the conditions

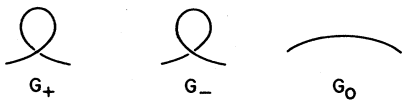

FIG. 13. The three line configurations considered in Eq. (2.15).

$$Q_{\text{unknot}}(\alpha,z)=1\ , \tag{2.14a}$$

$$Q_{G_\pm}(\alpha,z)=\alpha^{\mp 1}Q_{G_0}(\alpha,z)\ . \tag{2.15a}$$

It is related to $L(\alpha,z)$ by the relation (Lickorish, in Kauffman, 1990)

$$Q(\alpha,z)=-(-1)^{c(K)}i^{-w(K)}L(i\alpha,-iz)\ , \tag{2.16}$$

where $i=\sqrt{-1}$, $c(K)$ is the number of components of the knot K, and the writhe $w(K)$ is given by Eq. (2.1). Since the reversal of the orientation of one component of a link induces a change of writhe $\Delta w(K)=4n$, n being an integer, Eq. (2.16) is actually independent of the orientation chosen.

E. The semioriented invariant

Given an invariant of regular isotopy for unoriented knots, we can always use it to construct an invariant of ambient isotopy for oriented knots (Kauffman, 1988a). We state this result as a theorem:[4]

Theorem II.E. If $L(\alpha)$ is a polynomial of regular isotopy for an unoriented knot K satisfying Eqs. (2.14) and (2.15), then

$$F(\alpha)=\alpha^{-w(K)}L(\alpha) \tag{2.17}$$

is an invariant of ambient isotopy for an oriented knot derived from K. Here, w(K) is the writhe [Eq. (2.1)] of the oriented knot.

The proof of the theorem follows from the facts that both $w(K)$ and $L(\alpha)$ are regular isotopy invariants, i.e., invariant under Reidemeister moves II and III, and that the factor $\alpha^{-w(K)}$ in Eq. (2.17) cancels precisely those powers of α induced under Reidemeister moves I, to render $F(\alpha)$ ambient invariant.[5]

As examples, applying Theorem II.E to the bracket polynomial (Kauffman, 1987a; see Sec. V.B.2 below), one obtains the Jones polynomial, and applying it to the Kauffman polynomial, one obtains the F polynomial

$$F(\alpha,z)=\alpha^{-w(K)}L(\alpha,z)\ , \tag{2.18}$$

which is a two-variable polynomial of ambient isotopy

[3]Discovered by Kauffman is 1985 while visiting the city of Dubrovnik of the former Yugoslavia.

[4]Theorems are numbered by the sections in which they appear.

[5]Note that attaching orientations to configurations $G_\pm$ in Fig. 13 leads to the respective configurations $L_\mp$ for oriented knots, independent of the orienting direction chosen.

for oriented knots (Kauffman, 1990). A table of the F polynomials can be found in Lickorish and Millett (1988).

As a corollary, Theorem II.E implies that, when the orientation of one component of a link is reversed, the net results to the invariant $F(\alpha)$ is the introduction of an overall factor $\alpha^{-\Delta w(K)}$, where $\Delta w(K)$ is the change of writhe and is always in the form of $\Delta w(K)=4n$, n being an integer. For the Jones polynomial, for examples, we have $\alpha=-t^{-3/4}$ (Sec. V.B.2). Then the reversal of the orientation of one component introduces a factor t^{3n}, a fact verified by checking the list given in the Appendix. Since reversals of line orientations induce only changes of an overall factor, invariants given by Eqs. (2.17) and (2.18), including the Jones polynomial $V(t)$, have been termed "semioriented" (Lickorish, 1988; Lickorish and Millett, 1988).

III. LATTICE MODELS AND KNOT INVARIANTS

Lattice models are mathematical models of physical systems defined on lattices. While in the real world one deals with regular lattices of infinite size, many results on lattice models also hold for arbitrary finite lattices. It is these latter results that are useful in knot theory.

In lattice models one is interested in the computation of a partition function

$$Z=\sum W \tag{3.1}$$

where the summation is taken over all spin (or edge) states, and W is a Boltzmann factor defined for each configuration of spin (or edge) states. The Boltzmann factors are usually local in nature, that is, they can be decomposed into products of factors, each of which depends on states of few spins (edges) located in the immediate neighborhood. In statistical mechanics one further computes thermodynamic properties by taking derivatives of the partition function for infinite lattices. In knot theory, however, one deals mostly with partition functions.

The strategy of deriving knot invariants using statistical mechanics is the following: For each given knot, one constructs a two-dimensional lattice. One then seeks to construct lattice models on the lattice such that the partition function is identical for lattices constructed from equivalent knots. Then, by definition, the partition function is a knot invariant.

There are generally two different kinds of lattice models. If one places spins at lattice sites and introduces interactions among spins around an elementary cell of the lattice, one is led to spin models. This includes the special case of edge-interaction models for which only pair interactions are present. When there are multisite and/or hard-core interactions, the spin models are also known as interaction-round-a-face (IRF) models. Alternatively, if one places spins on lattice edges and associates weights with vertices according to the spin states of the incident edges, then one has vertex models. Vertex and IRF models are closely related and can always be transformed into each other (Perk and Wu, 1986a). For applications in knot theory, however, we shall see that it is convenient to begin with vertex models.

Historically, spin models originated from studies of the Ising model of ferromagnetism (Ising, 1925; Onsager, 1944). The study of vertex models was initiated in 1967 following Lieb's pioneering work on the exact determination of the residue entropy for square ice (Lieb, 1967a, 1967d), culminating in Baxter's exact solution of the two-state eight-vertex model (Baxter, 1971, 1972). The two-state vertex models have since been generalized to general q states (Kulish and Sklyanin, 1980, 1982; Schultz, 1981). The IRF model, a term coined by Baxter (1980), is another generalization of the eight-vertex model along a somewhat different route. A summary of early progress in lattice models can be found in the review by Lieb and Wu (1972) and the book by Baxter (1980). More recent results, particularly those on general q-state vertex and IRF models applicable to knot theory, are scattered through the literature.

The connection between knot theory and statistical mechanics was first noted by Jones (1985). In his derivation of the Jones polynomial, Jones noticed the resemblance of the von Neumann algebra used by him to the algebra occurring in the Temperley-Lieb formulation of the Potts model (Temperley and Lieb, 1971). The direct connection between the two seemingly unrelated fields came to light in 1986, when Kauffman (1987a) produced a remarkably simple derivation of the Jones polynomial using the bracket polynomial, a diagrammatic formulation which also arose in the consideration of the nonintersecting string model (Perk and Wu, 1986a) (see Sec. V.B.2 below). Soon thereafter, Jones worked out a derivation of the Homfly polynomial using a vertex-model approach. His derivation, while unpublished at the time, became widely known[6] and was extended by Turaev (1988) to the Kauffman polynomial. The connection of knot theory with statistical mechanics was formalized and further extended to include spin models by Jones (1989). Particularly, Jones introduced angle dependences to vertex models characterized by local weights.

The approach presented in this review follows closely that of Jones (1989). In particular, we consider vertex models with strictly local weights through the introduction of piecewise-linear lattices. We further establish that the IRF-model approach to knot invariants can be deduced as a special instance of the vertex-model formulation, thus simplifying the task of its derivation.

Finally, we point out the essence of the statistical mechanical approach. The statistical mechanical approach to knot invariants is based on the integrability of lattice models. Since we are seeking lattice models whose partition functions are invariant under Reidemeister moves, the main idea is that the partition function of integrable models (in the infinite-rapidity limit) naturally

[6]See example 1.16 in Jones (1989).

fulfills the requirement of Reidemeister moves IIIA (see Sec. V.A.1 below), a point not readily seen in the braid-group approach (Jones, 1990b). In addition, Reidemeister move IIA is satisfied as a consequence of unitarity. It is then a relatively simple matter to require the invariance of the partition function only under Reidemeister moves I and IIB.

Our main results are summarized in Theorems V.A.1 (for vertex models), VI.F (for IRF models), and VII.A (for models with pure two-spin interactions).

IV. VERTEX MODELS

A. Formulation

Consider a finite lattice $\mathcal{L}$ of N sites (vertices), E edges, and arbitrary shape. For our purposes we shall confine ourselves to lattices with a uniform coordination number and without free edges, i.e., every edge terminates at two vertices. An example of one such lattice is shown in Fig. 14.

Place spins on lattice edges, and let each spin independently take on q distinct values, or states. It is often convenient to associate colors with spin states so that one may regard edges as being colored. Then the partition function Z in Eq. (2.1) generates q^E edge colorings of $\mathcal{L}$. In the case of $q=2$, for example, one may regard the edges as having two colors, and thus one is led to consider two-state vertex models that have been analyzed extensively (for reviews see Lieb and Wu, 1972, and Baxter, 1980).

In vertex models the Boltzmann factor in Eq. (3.1) is taken to be a product of individual vertex weights, and the partition function reads

$$Z_{\text{vertex}}(\omega)=\sum_{\{\text{edge states}\}}\prod_{i=1}^{N}\omega_i\ , \tag{4.1}$$

where ω_i, the vertex weight of the ith vertex, is a function of the spin states of its four incident edges.

Since we have arbitrary lattices in mind, in which vertices can assume arbitrary orientations, a local frame of reference is needed to properly define the weights. This can be provided by directing lattice edges such that each vertex is formed by the crossing of two directed lines. For example, the lattice in Fig. 14 can be directed as shown in Fig. 15. We can now write the vertex weight as

FIG. 14. A finite lattice of coordination number four. The lattice contains 6 vertices and 12 edges.

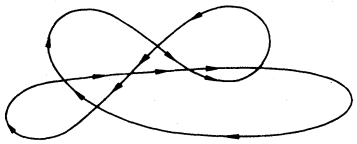

FIG. 15. A directed lattice.

$$\omega_i=\omega_i(a,b|x,y)=\omega_i\begin{bmatrix} y & b \\ a & x \end{bmatrix}\ , \tag{4.2}$$

where a, b, x, y are numerical numbers denoting the spin states of the four incident edges of a vertex as arranged in Fig. 16. We shall assume the indices $\{a,b,x,y\}\in\mathcal{J}$, where $\mathcal{J}$ is a set of q numerical values distributed *symmetrically* about zero.

In the most general case, Eq. (4.2) gives rise to q^4 distinct vertex weights and a q^4-vertex model. For $q=2$, for example, this becomes the 16-vertex model (Lieb and Wu, 1972). Several special case cases of the $q=2$ problem have been considered in the past; these include the six-vertex (Lieb, 1967a, 1967b, 1967c; Sutherland, 1967) and the eight-vertex (Fan and Wu, 1970; Baxter, 1971, 1972) models.

B. The Yang-Baxter equation

The q^4-vertex model is *integrable* if the q^4 vertex weights satisfy a condition known as the *Yang-Baxter equation.* In practice, integrability of lattice models often leads to closed-form solutions of the partition function and other physical quantities such as correlation functions. For our purposes, however, it suffices to consider only solutions of the Yang-Baxter equation, which, as we shall see, lead naturally to the realization of type-IIIA Reidemeister moves. As alluded to earlier in Sec. III, this is the key to the statistical mechanical derivation of knot invariants.

Consider two clusters of lattice edges containing three lattice sites represented by the upward-pointing and downward-pointing triangles in Fig. 17. The Yang-Baxter equation is the condition on the vertex weights such that the partition functions of these two small lattices are identical for any given states $\{a,b,c,d,e,f\}$. This implies that one may replace an upward-pointing triangle that is part of a lattice by a downward-pointing one, and vice versa, without affecting the overall partition function. Algebraically, this condition reads

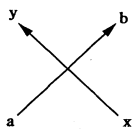

FIG. 16. The orientation of a vertex.

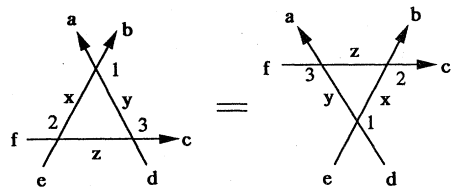

FIG. 17. The Yang-Baxter equation for vertex models.

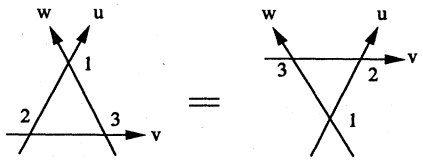

FIG. 18. Association of rapidities u, v, w, with the lines.

$$\sum_{x,y,z\in\mathcal{J}} \omega_1(x,b|y,a)\omega_2(f,z|e,x)\omega_3(z,c|d,y)=\sum_{x,y,z,\in\mathcal{J}} \omega_1(e,x|d,y)\omega_2(z,c|x,b)\omega_3(f,z|y,a)$$

$$\text{for all } a,b,c,d,e,f\in\mathcal{J}\ . \qquad (4.3)$$

Here, we have allowed vertex weights to be different at the three sites.

Historically, the Yang-Baxter equation arose for $q=2$ as the factorizability condition in the Bethe-ansatz approach to the one-dimensional delta-function gas [McGuire (1964) for the Bose gas considered by Lieb and Liniger (1963); Gaudin (1967) and Yang (1967) for the Fermi gas] and as the star-triangle relation in solvable two-dimensional models in statistical mechanics [Onsager (1944) for the Ising model; Baxter (1972) for the eight-vertex model; Baxter (1978) for the general Z-invariant model]. The Yang-Baxter equation, a term introduced by the Faddeev school,[7] also arises in the theory of the factorized S matrix in quantum field theory (Zamolodchikov, 1979), for which the vertex weight ω is known as the R matrix. For general q, a problem first studied by Kulish and Sklyanin (1980, 1982) and Schultz (1981), Eq. (4.3) is a set of q^6 equations with $3\times q^4$ unknowns and is highly overdetermined.

The most general solution of the Yang-Baxter equation is not yet known, but families of solutions, including many of the special solutions found by brute force, can be constructed by using finite-dimensional representations of simple Lie algebras (Bazhanov, 1985; Jimbo, 1986) connected with quantum groups (Drinfel'd, 1986). These solutions are parametrized by assigning line variables, or rapidities (spectral parameters), u, v, w to the three lines, as shown in Fig. 18, so that one has

$$\begin{aligned}\omega_1(a,b|x,y)&=\omega(a,b|x,y|u-w)\\&=\omega\begin{bmatrix}y & b\\ a & x\end{bmatrix}(u-w)\ ,\\ \omega_2(a,b|x,y)&=\omega(a,b|x,y|v-u)\ ,\\ \omega_3(a,b|x,y)&=\omega(a,b|x,y|v-w)\ .\end{aligned} \qquad (4.4)$$

That is, vertex weights depend on a parameter that is the difference of the two rapidities of the two lines crossing at each vertex. Furthermore, it can be shown (Perk and Wu, 1986b) that the decoupling (initial) condition

$$\omega(a,b|x,y|0)=\delta_{ay}\delta_{bx} \qquad (4.5a)$$

usually satisfied by solutions of the Yang-Baxter equation leads to the unitarity condition

$$\sum_{b,y\in\mathcal{J}} \omega(a,b|x,y|v-u)\omega(y,z|b,c|u-v)=\delta_{ac}\delta_{xz}\ , \qquad (4.5b)$$

a situation shown in Fig. 19. Here, the Kronecker delta indicates that there is a contribution only when the two lines have identical indices. Solutions of the Yang-Baxter equation useful in constructing knot invariants are those with trigonometric parametrizations, usually the degenerate critical manifolds of more general soluble families with elliptic function parametrizations. This leads, as we shall see, to various generalizations of the two-state six-vertex models solved by Lieb (1967c, 1967d) to general q states.

The infinite rapidity limit. In pursuing realizations of knots as vertex models, we need two kinds of vertex weights for the + and − types of crossings. This need can be fulfilled by taking the infinite-rapidity limit $u\to\infty$, $v\to\infty$, $w\to\infty$ and writing[8]

$$\omega_\pm\begin{bmatrix}c & d\\ a & b\end{bmatrix}\equiv\lim_{u\to\pm\infty}\omega\begin{bmatrix}c & d\\ a & b\end{bmatrix}(u)\ . \qquad (4.6)$$

Here it is understood that the right-hand side of Eq. (4.6) has been divided by a divergent factor, such as $\sinh u$ or $e^{\beta|u|}$ where β is a constant, such that only the leading weights contribute. The less divergent weights, if any, vanish in this limit.

Then, depending on the relative magnitudes of u, v, w, the Yang-Baxter equation (4.3) reduces to six different equations shown schematically in Fig. 20. These are given by Eq. (4.3) with indices

[7]The term *Baxter-Yang relation* first appeared in a review on the quantum inverse scattering method by Takhtadzhan and Faddeev (1979), and the name *Yang-Baxter equation* was used thereafter by the Faddeev school. A useful collection of relevant reprints on the Yang-Baxter equation can be found in Jimbo (1989).

[8]The subscripts ± and the argument u of a vertex weight ω serve to remind us that ω is a solution of the Yang-Baxter equation.

$$\{1,2,3\}=\{--+\},\{-++\},\{---\},\{+--\},\{+++\},\{+-+\}\ . \tag{4.7}$$

It is intriguing to note that the six configurations specified by Eq. (4.7) coincide precisely with those in Fig. 5 representing the six possible Reidemeister moves IIIA. Similarly, the unitarity relation Eq. (4.5b) reduces to

$$\sum_{b,y\in\mathcal{J}} \omega_{\pm}(a,b|x,y)\omega_{\mp}(y,z|b,c)=\delta_{ac}\delta_{xz}\ , \tag{4.8}$$

represented by configurations coinciding with that of Reidemeister move IIA shown in Fig. 4. Conversely starting from a given $\omega_{\pm}\equiv\omega(\pm\infty)$ obtained from, say, braid-group analysis, one may seek to reconstruct the weight $\omega(u)$. This inverse process is termed *Baxterization* (Jones, 1990b).

C. Enhanced vertex models

It often happens that vertex weights occurring in a vertex model contain factors depending explicitly on angles between the incident lattice edges, a local parameter that may vary from vertex to vertex. It further transpires that one often regroups these local factors according to global loops, a technique first used in an analysis of the Potts model by Baxter *et al.* (1976) for arbitrary two-dimensional lattices. It is then convenient to replace curved edges, such as those shown in Fig. 15, by zigzag lines. This leads to the consideration of *piecewise-linear* lattices $\mathcal{L}^*$. For example, the conversion of the oriented lattice in Fig. 15 into one that is piecewise linear is shown in Fig. 21. Note that the conversion creates new vertices of degree 2.

Consider next an *enhanced* vertex model on $\mathcal{L}^*$ derived from the vertex model on $\mathcal{L}$ by associated angle dependences with vertex weights. For vertices of degree two, shown in Figs. 22(a) and 22(b), we associate vertex weights

$$\begin{aligned}\omega^*(a)=\lambda^{a\theta/2\pi}&\text{ if the line turns an angle }\theta\\ &\text{to the left ,}\\ =\lambda^{-a\theta/2\pi}&\text{ if the line turns an angle }\theta\\ &\text{to the right ,}\end{aligned} \tag{4.9}$$

where a is the state variable, and λ a variable yet to be specified.[9] The product of the vertex weights $\omega^*(a)$ along the zigzag path shown in Fig. 23 is given by

$$\prod_{\text{path}} \omega^*(a)=\lambda^{a(-\theta_1+\theta_2+\cdots)}=\lambda^{a\theta/2\pi}\ , \tag{4.10}$$

where θ is the angle between the final and initial directions of the path. Thus one always obtains the same product, independent of the way that the curved edges are linearized. In addition, the creation of vertices of degree 2 leads to the consideration of lattices in the shape of a ring. Since the product of vertex weights along a ring is

$$\begin{aligned}\prod_{\text{closed path}} \omega^*(a)=\lambda^a&\text{ arrows in counterclockwise}\\ &\text{direction ,}\\ =\lambda^{-a}&\text{ arrows in clockwise direction ,}\end{aligned} \tag{4.11}$$

the partition function of a ring,

$$Z_{\text{ring}}(\omega^*)=\sum_{\alpha\in\mathcal{J}}\lambda^a\ , \tag{4.12}$$

is independent of the arrow direction for $\mathcal{J}$ symmetric about zero.

In the same spirit, we modify all other vertex weights by multiplying them by a factor to yield the angle-dependent weights

$$\begin{aligned}\omega^*(a,d|b,c|u)&\equiv\omega^*\begin{bmatrix}c & d\\ a & b\end{bmatrix}(u)\\ &=\lambda^{(a+c-b-d)\theta/4\pi}\omega(a,d|b,c|u)\end{aligned} \tag{4.13a}$$

and the infinite-rapidity limits

$$\omega^*_{\pm}(a,d|b,c)=\lambda^{(a+c-b-d)\theta/4\pi}\omega_{\pm}(a,d|b,c)\ , \tag{4.13b}$$

where a, b, c, d are arranged as shown in Fig. 22(c), and θ is the angle between the two incoming (or outgoing) arrows.[10] Explicitly, the partition function of the enhanced

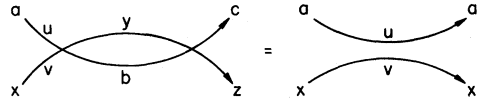

FIG. 19. The unitarity condition for vertex weights.

[9]Since λ is as yet unspecified, we may write λ^a as λ^{h_a} for some function h_a indexing the lattice edge. Then the discussions of this section and Sec. IV.D below can be carried through, provided that we replace the condition $a+b=c+d$ in Eq. (4.16) by $h_a+h_b=h_c+h_d$, and the factor $a-d$ in the exponent in Eq. (4.18) by h_a-h_d. This generalization proves to be useful when vertex-model results are applied to IRF models in Sec. VII.

[10]We shall assume that all vertices are formed by the crossing of two straight lines, so that $0<\theta<\pi$.

vertex model is

$$Z_{\text{vertex}}(\omega^*)=\sum_{\{\text{edge states}\}}\prod\omega^*(a,b|x,y|u)\prod\omega^*(a)\ , \tag{4.14a}$$

and, in the infinite-rapidity limit,

$$Z_{\text{vertex}}(\omega_\pm^*)=\sum_{\{\text{edge states}\}}\prod\omega_\pm^*(a,b|x,y)\prod\omega^*(a)\ , \tag{4.14b}$$

where the two products are taken over vertices of degrees 4 and 2, respectively.

For the enhanced vertex model to be useful in knot theory, we require the *enhanced* Yang-Baxter equation

$$\sum_{x,y,z\in\mathcal{J}}\omega^*(x,b|y,a|u-w)\omega^*(f,z|e,x|v-u)\omega^*(z,c|d,y|v-w)$$
$$=\sum_{x,y,z,\in\mathcal{J}}\omega^*(e,x|d,y|u-w)\omega^*(z,c|x,b|v-u)\omega^*(f,z|y,a|v-w) \tag{4.15}$$

to hold. This leads us to consider charge-conserving models.

D. Charge-conserving vertex models

In most of our applications we shall have

$$\omega\begin{bmatrix}c & d\\ a & b\end{bmatrix}(u)=0 \quad \text{unless } a+b=c+d\ . \tag{4.16}$$

If we regard the functions a, b, c, d as defining charges with edges, then the total charge of incoming/outgoing arrows is conserved, and we refer to Eq. (4.16) as the condition of *charge conservation.* In charge-conserving models the angle-dependent weights, Eqs. (4.13a) and (4.13b), are, respectively,

$$\omega^*(a,d|b,c|u)=\omega^*\begin{bmatrix}c & d\\ a & b\end{bmatrix}(u)$$
$$=\lambda^{(a-d)\theta/2\pi}\omega(a,d|b,c|u)\ , \tag{4.17a}$$

$$\omega_\pm^*(a,d|b,c)=\omega_\pm^*\begin{bmatrix}c & d\\ a & b\end{bmatrix}$$
$$=\lambda^{(a-d)\theta/2\pi}\omega_\pm\begin{bmatrix}c & d\\ a & b\end{bmatrix}\ . \tag{4.17b}$$

Using the identity $\theta_3=\theta_1+\theta_2$, where θ_i is the angle between the two incoming arrows at site i in Fig. 18, one can readily verify that the vertex weight Eq. (4.17a) is a solution of the enhanced Yang-Baxter equation (4.15), provided that $\omega(a,d,|b,c|u)$ is a solution of the Yang-Baxter equation (4.3). It follows that Eq. (4.17b) is the solution of Eq. (4.15) in the infinite-rapidity limit. Along the same lines, since the rapidity differences also satisfy $u_3=u_1+u_2$, where u is the difference of the two rapidities at site i,

$$\tilde{\omega}(a,d,|b,c|u)\equiv e^{\beta(a-d)u}\omega(a,d,|b,c|u)\ , \tag{4.18}$$

where β is arbitrary, is also a solution of the Yang-Baxter equation. This is a "symmetry-breaking" transformation, which provides to be useful in latter applications. We shall leave open the possibility of introducing this

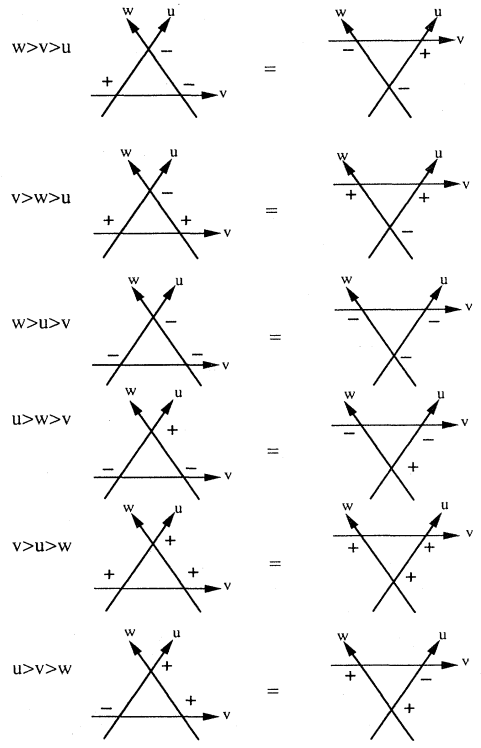

FIG. 20. The Yang-Baxter equation in the infinite-rapidity limit.

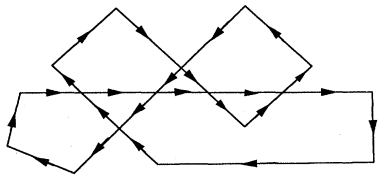

FIG. 21. A directed piecewise-linear lattice.

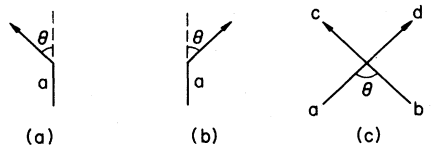

FIG. 22. Vertices in piecewise-linear lattices.

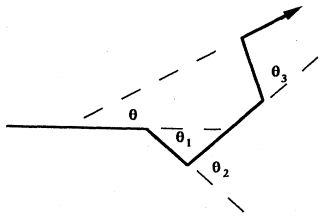

FIG. 23. A directed path.

symmetry breaking and use ω to denote either ω or $\bar{\omega}$, whichever is needed in the application.

E. Integrable vertex models

We now present examples of integrable vertex models known in statistical mechanics.

1. The spin-conserving model

Schultz (1981) and Perk and Schultz (1981, 1983) have carried out a systematic study of solutions of the Yang-Baxter equation in some special cases. The first case is a $q(2q-1)$-vertex model generalizing the $(q=2)$ six-vertex ice-type models (Lieb, 1967a, 1967b, 1967c). In this vertex model all weights vanish except those associated with the $q(2q-1)$ configurations shown in Fig. 24. If one identifies edge variables as spins, then the incoming/outgoing spins are conserved,[11] that is, we have either

$$\{a=c,\ b=d\} \quad \text{or} \quad \{a=d,\ b=c\} \ . \tag{4.19}$$

Thus the spin-conserving model satisfies charge conservation, $a+b=c+d$. For $q=2$, the condition (4.19) is equivalent to the ice rule (Wu, 1967, 1968) leading to the six-vertex models solved by Lieb (1967a, 1967b, 1967c).

Let W_{aa}, S_{ab}, and T_{ab}, $a\neq b$, be the vertex weights shown in Fig. 24. Then we can write

$$\omega\begin{bmatrix} c & d \\ a & b \end{bmatrix}(u)=W_{aa}(u)\delta_{abcd}+S_{ab}(u)(\delta_{ad}\delta_{bc}-\delta_{abcd}) + T_{ab}(u)(\delta_{ac}\delta_{bd}-\delta_{abcd}) \ , \tag{4.20}$$

where δ_{ab} is the Kronecker delta function and

$$\delta_{abcd}=1 \ \text{ if } a=b=c=d \ , \quad =0 \ \text{ otherwise} \ . \tag{4.21}$$

Perk and Schultz (1983) found that, within the family of Eq. (4.20), the solution of the Yang-Baxter equation is, excluding an overall normalization,[12]

$$W_{aa}(u)=\sinh(\eta+\epsilon_a u) \ , \quad S_{ab}(u)=\sinh u \ , \quad T_{ab}(u)=e^{-u[\mathrm{sgn}(a-b)]}\sinh\eta \ , \tag{4.22}$$

where $\epsilon_a=1$ or -1, and η is arbitrary. In the infinite-rapidity limit, Eqs. (4.20) and (4.22) become

$$\omega_{\pm}\begin{bmatrix} c & d \\ a & b \end{bmatrix}=A_{\pm}(\epsilon_a e^{\pm\epsilon_a\eta}\delta_{abcd}+(\delta_{ad}\delta_{bc}-\delta_{abcd}) \pm(e^{\eta}-e^{-\eta})\theta[\pm(b-a)]\delta_{ac}\delta_{bd}) \ , \tag{4.23}$$

where we have divided the weight, Eq. (4.20), by $\sinh u$ and introduced normalization factor $A_{\pm}$ and the step function

$$\theta(b-a)=1 \ \text{ if } b>a \ , \quad =0 \ \text{ if } b\leq a \ . \tag{4.24}$$

It is instructive to write out Eq. (4.23) explicitly. Excluding the normalization factor $A_{\pm}$, we have

$$\begin{aligned} &\omega_{\pm}\begin{bmatrix} a & a \\ a & a \end{bmatrix}=\epsilon_a e^{\pm\epsilon_a\eta} \ , \\ &\omega_{\pm}\begin{bmatrix} b & a \\ a & b \end{bmatrix}=1, \quad a\neq b \ , \\ &\omega_{+}\begin{bmatrix} a & b \\ a & b \end{bmatrix}=e^{\eta}-e^{-\eta}, \quad a<b \ , \\ &\omega_{-}\begin{bmatrix} a & b \\ a & b \end{bmatrix}=-(e^{\eta}-e^{-\eta}), \quad a>b \ , \\ &\omega_{\pm}\begin{bmatrix} c & d \\ a & b \end{bmatrix}=0, \quad \text{otherwise} \ . \end{aligned} \tag{4.25}$$

As we shall see, this spin-conserving model leads to the Homfly polynomial.

2. The N-state vertex model

Another family of integrable charge-conserving models is the N-state vertex model (Sogo *et al.*, 1983). Let the edge variables take on N distinct values,

[11]The term *spin conservation* has been used by different authors in different contexts. Here we use it to refer to models in which the states of the incoming and outgoing arrows are strictly the same.

[12]Here we have omitted some multiplication factors corresponding to gauge transformations and external fields that do not concern us.

$$\mathcal{J}=\left\{-\left[\frac{N-1}{2}\right],-\left[\frac{N-3}{2}\right],\ldots,\left[\frac{N-3}{2}\right],\left[\frac{N-1}{2}\right]\right\}, \tag{4.26}$$

for fixed $N=2,3,\ldots$. Then the N-state vertex model is specified by

$$a+b=c+d=l,\quad |l|\le N-1\ , \tag{4.27}$$

that is, charge-conserving weights with the total charge $l\le N-1$. This yields a total of $2\sum_{l=0,1,2,\ldots}^{N-1} l^2+N^2=N(2N^2+1)/3$ vertex configurations, leading to the 6-vertex (ice-type) models for $N=2$ and the 19-vertex model (Zamolodchikov and Fateev, 1980) for $N=3$. For example, the $N=2$ solution is (Akutsu and Wadati, 1987b)

$$\begin{aligned}
&\omega\begin{bmatrix}\frac12&\frac12\\ \frac12&\frac12\end{bmatrix}(u)=\omega\begin{bmatrix}-\frac12&-\frac12\\ -\frac12&-\frac12\end{bmatrix}(u)=\sinh(\eta-u)\ ,\\
&\omega\begin{bmatrix}\frac12&-\frac12\\ -\frac12&\frac12\end{bmatrix}(u)=\omega\begin{bmatrix}-\frac12&\frac12\\ \frac12&-\frac12\end{bmatrix}(u)=\sinh u\ ,\\
&\omega\begin{bmatrix}\frac12&-\frac12\\ \frac12&-\frac12\end{bmatrix}(u)=e^{-u}\sinh\eta\ ,\\
&\omega\begin{bmatrix}-\frac12&\frac12\\ -\frac12&\frac12\end{bmatrix}(u)=e^{u}\sinh\eta\ ,
\end{aligned} \tag{4.28}$$

where the vertex weights are those including the symmetry-breaking factor in Eq. (4.18) with $\beta=1$. We observe that this solution is identical to that of the spin-conserving model given by Eqs. (4.20) and (4.22) with $q=2$, $\epsilon_a=-1$. But the general N-state vertex model is different from the spin-conserving model. Explicit expressions of vertex weights for $N=3,4$ can be found in Sogo *et al.* (1983) and Akutsu and Wadati (1987b). The general N model can be constructed using, for example, a fusion procedure (Kulish and Sklyanin, 1982b) according to the ideas of Kulish *et al.* (1981).

An expression for vertex weights $\omega_\pm$, the infinity-rapidity limit of $w(u)$, for general N has been given by Jones (1989). This expression, which includes the symmetry-breaking factor in Eq. (4.18) with $\beta=1$ and reduces to our $\epsilon_a=1$ solution in the case of $N=2$, is

$$\omega_+\begin{bmatrix}c&d\\ a&b\end{bmatrix}(\eta)=e^{\eta[(ab+cd)+k(k-1)/2]}\times\Gamma^N_{b,k}(\eta)[\theta(a-b)+\delta_{ab}]\ , \tag{4.29}$$

where $k=a-d$,

$$\Gamma^N_{b,k}(\eta)=\prod_{n=0}^{k-1}\left[\frac{2\sinh[(b+n+\frac12 N+\frac12)\eta]\sinh[(b+n-\frac12 N-\frac12)\eta]}{-\sinh[(n+1)\eta]}\right], \tag{4.30}$$

with empty product being 1, and

$$\omega_-\begin{bmatrix}c&d\\ a&b\end{bmatrix}(\eta)=\omega_+\begin{bmatrix}d&c\\ b&a\end{bmatrix}(-\eta)\ . \tag{4.31}$$

This vertex model leads to the Akutsu-Wadati polynomial.

3. The nonintersecting-string model

Another family of solutions considered by Perk and Schultz (1983) is the $q(2q-1)$-vertex model with vertex weights shown in Fig. 25. These are vertex weights characterized by either

$$\{a=c,\ b=d\}\ \text{ or }\ \{a=b,\ c=d\}\ . \tag{4.32}$$

Thus the vertex weight is

$$\omega\begin{bmatrix}c&d\\ a&b\end{bmatrix}(u)=W_{aa}(u)\delta_{abcd}+S_{ab}(u)(\delta_{ab}\delta_{cd}-\delta_{abcd})+T_{ab}(u)(\delta_{ac}\delta_{bd}-\delta_{abcd})\ . \tag{4.33}$$

If at each vertex we connect edges in the same states, then the partition function (4.1) generates polygons on $\mathcal{L}$ that do not intersect. Hence this is a model of nonintersecting strings. For $q=2$, this reduces to a six-vertex

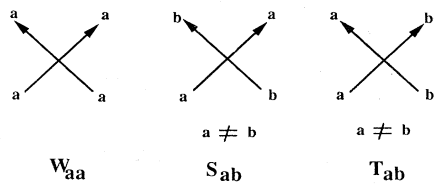

FIG. 24. Vertex weights of the spin-conserving vertex model.

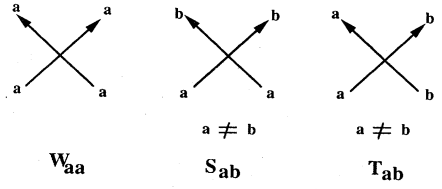

FIG. 25. Vertex weights of the nonintersecting-string model.

model discussed by Lieb and Wu (1972). Two models for $q=3$ have been considered by Stroganov (1979). Note that the nonintersecting-string model does not obey the charge-conserving condition,[13] Eq. (4.16), and consequently we take $\lambda=1$ so that all vertices of degree two in $\mathcal{L}^*$ have the weight

$$\omega(a)=1, \quad \text{for all } a \ . \tag{4.34}$$

Perk and Schultz (1981, 1983) found that there exist exactly $q+1$ distinct integrable models in the form of Eq. (4.33). One of the integrable cases, termed the separable model by Perk and Wu (1986a), is

$$\begin{aligned} W_{aa}(u)&=\sinh u+\sinh(\eta-u) \ , \\ S_{ab}(u)&=\sinh u \ , \\ T_{ab}(u)&=\sinh(\eta-u) \ . \end{aligned} \tag{4.35}$$

In the infinite-rapidity limit, we obtain from Eq. (4.33)

$$\omega_\pm \begin{bmatrix} c & d \\ a & b \end{bmatrix} = A_\pm[\delta_{ab}\delta_{cd}-e^{\mp\eta}\delta_{ac}\delta_{bd}] \ , \tag{4.36}$$

where we have again divided Eq. (4.33) by $\sinh u$ and included a normalization factor $A_\pm$. Explicitly, excluding the normalization factor $A_\pm$, we have

$$\begin{aligned} \omega_\pm \begin{bmatrix} a & a \\ a & a \end{bmatrix} &= 1-e^{\pm\eta} \ , \\ \omega_\pm \begin{bmatrix} a & b \\ a & b \end{bmatrix} &= -e^{\pm\eta}, \quad a\neq b \ , \\ \omega_\pm \begin{bmatrix} a & a \\ b & b \end{bmatrix} &= 1, \quad a\neq b \ , \\ \omega_\pm \begin{bmatrix} c & d \\ a & b \end{bmatrix} &= 0, \quad \text{otherwise} \ . \end{aligned} \tag{4.37}$$

As we shall see, this vertex model leads to the Jones polynomial (Lipson, 1992; Wu, 1992b).

V. KNOT INVARIANTS FROM VERTEX MODELS

A. Oriented knots

1. Formulation

Starting from a given oriented knot, one constructs a directed lattice $\mathcal{L}$ and the associated piecewise-linear lattice $\mathcal{L}^*$ by regarding lines of the knot as lattice edges and line crossings as lattice sites (vertices). This leads naturally to two types of vertices, + and −, corresponding to the two kinds of line crossings + and −. For example, from a trefoil one constructs the directed lattice in Fig. 26 and the piecewise-linear lattice in Fig. 27, both having three + crossings.

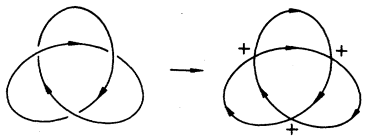

FIG. 26. Construction of a lattice from a knot.

We next seek to construct an enhanced vertex model on $\mathcal{L}^*$ with correspondingly two different kinds of vertex weights $\omega_\pm^*$, such that its partition function $Z(\omega_\pm^*)$ is a knot invariant. That is, we require $Z(\omega_\pm^*)$ to remain invariant under Reidemeister moves of the lattice edges. To accomplish this, we use vertex weights $\omega_\pm^*$ derived from the enhanced Yang-Baxter equation (4.15). Indeed, as remarked after Eq. (4.7), configurations of the Yang-Baxter equation in the infinite-rapidity limits coincide precisely with those of type-IIIA Reidemeister moves. As a result, the partition function $Z(\omega_\pm^*)$ is *by definition* invariant under type-IIIA moves. We therefore need only examine its invariance under Reidemeister moves I and II (moves IIIB follow as a consequence). Note that the use of the infinite-rapidity limit, Eq. (4.6), a crucial step whose meaning is not well understood in the braid-group approach (Witten, 1989b; Jones, 1990b), now emerges naturally as a condition for ensuring invariance under Reidemeister moves IIIA.

The invariance of $Z(\omega_\pm^*)$ under Reidemeister moves I, shown in Fig. 28, reads

$$\sum_{a\in\mathcal{J}} \lambda^{a(2\pi-\theta)/2\pi}\omega_\pm^*(a,b\,|x,a)=\lambda^{-b\theta/2\pi}\delta_{bx} \quad \text{(I)} \ , \tag{5.1}$$

where we have used the identity $\theta_1+\theta_2+\theta_3=2\pi-\theta$. Similarly, consideration of the invariance of $Z(\omega_\pm^*)$ under Reidemeister moves IIA and IIB, shown in Figs. 29 and 30, respectively, leads to the conditions

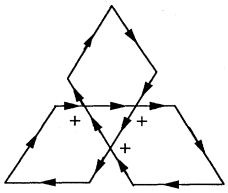

FIG. 27. The piecewise-linear lattice constructed from the lattice in Fig. 26.

[13]However, by applying a staircase-type transformation generalizing the one used by Fan and Wu (1970) for the eight-vertex model, one can view the nonintersecting-string model as a checkerboard spin-conserving model. I am indebted to J. H. H. Perk for this remark.

$$\sum_{b,y\in\mathcal{J}} \lambda^{(b-y)\theta/2\pi}\omega_{\pm}^{*}(a,b|x,y)\omega_{\mp}^{*}(y,z|b,c)$$
$$=\lambda^{(a-x)\theta/2\pi}\delta_{ac}\delta_{xz} \quad \text{(IIA)}, \tag{5.2}$$
$$\sum_{b,y\in\mathcal{J}} \lambda^{(y+b)(\pi-\theta)/2\pi}\omega_{\pm}^{*}(y,x|a,b)\omega_{\mp}^{*}(b,c|z,y)$$
$$=\lambda^{(a+x)(\pi-\theta)/2\pi}\delta_{xz}\delta_{ac} \quad \text{(IIB)}. \tag{5.3}$$

For completeness, although it is redundant, we write down the requirement imposed by Reidemeister moves IIIB. Using the labelings shown in Fig. 31, we have

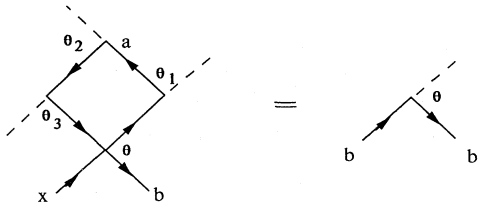

FIG. 28. Labelings for Reidemeister moves I.

$$\sum_{x,y,z\in\mathcal{J}} \omega_1^{*}(y,a|b,x)\omega_2^{*}(x,c|f,z)\omega_3^{*}(z,c|d,y)=\sum_{x,y,z\in\mathcal{J}} \omega_1^{*}(d,y|x,e)\omega_2^{*}(b,c|z,c)\omega_3^{*}(f,z|y,a) \quad \text{(IIIB)}, \tag{5.4}$$

$$\{1,2,3\}=\{+--\},\{+-+\},\{++-\},\{-+-\},\{---+\},\{-++\}. \tag{5.5}$$

For charge-conserving models, we use Eqs. (4.17a) and (4.17b) and obtain from Eqs. (5.1)–(5.3) the equivalent conditions

$$\sum_{a\in\mathcal{J}} \lambda^{a}\omega_{\pm}(a,b|x,a)=\delta_{bx}, \quad \text{(I)}, \tag{5.1a}$$

$$\sum_{b,y\in\mathcal{J}} \omega_{\pm}(a,b|x,y)\omega_{\mp}(y,z|b,c)=\delta_{ac}\delta_{xz} \quad \text{(IIA)}, \tag{5.2a}$$

$$\sum_{b,y\in\mathcal{J}} \lambda^{b-a}\omega_{\pm}(y,x|a,b)\omega_{\mp}(b,c|z,y)=\delta_{xz}\delta_{ac} \quad \text{(IIB)}. \tag{5.3a}$$

Here, $\omega_{\pm}(a,b,|c,d)$ are defined by Eqs. (4.6) and (4.4) and are deduced from the solution of the Yang-Baxter equation (4.3). These are the *fundamental* conditions, which do not refer to enhanced weights. Note that they do not depend on the angle θ and the condition (5.2a) coincides with the unitarity relation, Eq. (4.8).

We now collect our main results and state them as a theorem:

Theorem V.A.1. For each oriented knot construct a directed lattice $\mathcal{L}$ and the associated piecewise-linear lattice $\mathcal{L}^{*}$. Then the partition function (4.14b), with vertex weights $\omega^{*}(a)$ given by Eq. (4.9) and $\omega_{\pm}^{*}$ by the infinite-rapidity limit of the solution of the enhanced Yang-Baxter equation (4.15), is a knot invariant, provided that Eqs. (5.1)–(5.3) hold.

For charge-conserving models, $\omega_{\pm}^{*}$ is given by Eq. (4.17b), and Eqs. (5.1)–(5.3) reduce to the fundamental conditions (5.1a)–(5.3a).

Skein relation. With knot invariants formulated as partition functions, Skein relations relating knot invariants can be formulated in terms of vertex weights. For the Homfly polynomial, for example, it is readily verified that the Skein relation (2.8) is equivalent to the following relation among the enhanced vertex weights:

$$t^{-1}\omega_{+}^{*}\begin{bmatrix} c & d \\ a & b \end{bmatrix}-t\omega_{-}^{*}\begin{bmatrix} c & d \\ a & b \end{bmatrix}=z\lambda^{(a-d)\theta/2\pi}\delta_{ac}\delta_{bd}. \tag{5.6}$$

For charge-conserving models Eq. (5.6) reduces to

$$t^{-1}\omega_{+}\begin{bmatrix} c & d \\ a & b \end{bmatrix}-t\omega_{-}\begin{bmatrix} c & d \\ a & b \end{bmatrix}=z\delta_{ac}\delta_{bd}. \tag{5.6a}$$

Similar relations can be written down for other Skein relations.

We now apply our formulation to obtain knot invariants.

2. The Homfly polynomial

We now show that the q-state spin-conserving model described in Sec. IV.E.1 (Perk and Schultz, 1981, 1983) generates the Homfly polynomial (Jones, 1989). The vertex weights $\omega_{\pm}^{*}$ of the spin-conserving model are given by

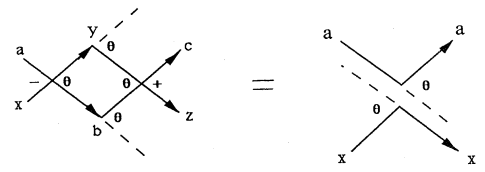

FIG. 29. Labelings for Reidemeister moves IIA.

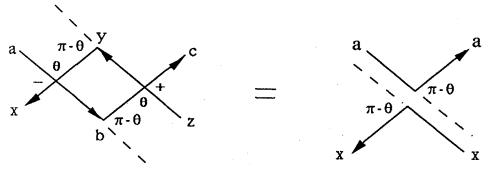

FIG. 30. Labelings for Reidemeister moves IIB.

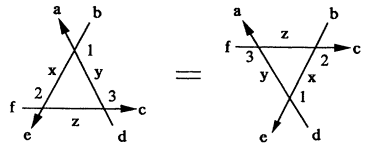

FIG. 31. Labelings for Reidemeister moves IIIB.

Eqs. (4.20) and (4.23) with[14]

$$\epsilon_a=-1 \quad \text{for all } a \ , \tag{5.7}$$

and

$$\mathcal{J}=\{-(q-1),-(q-3),\ldots,(q-3),(q-1)\} \ , \tag{5.8}$$

containing q integers with intervals of 2 in between.

The partition function is invariant under Reidemeister moves IIIA by construction. To satisfy invariance under Reidemeister moves I, we substitute the vertex weight (4.23) with $\epsilon_a=-1$ in Eq. (5.1a) and obtain

$$A_\pm\left[-e^{\mp\eta}\lambda^b\pm(e^\eta-e^{-\eta})\sum_{a\in\mathcal{J}}\theta[\pm(b-a)]\lambda^a\right]=1, \quad b\in\mathcal{J} \ . \tag{5.9}$$

Using the identity

$$\sum_{a\in\mathcal{J}}\theta[\pm(b-a)]\lambda^a=(\lambda^{\mp(q-1)}-\lambda^b)/(1-\lambda^{\pm 2}) \ , \tag{5.10}$$

we deduce from Eq. (5.9) the condition

$$A_\pm e^{\pm\eta}\left[\lambda^b+\frac{(1-e^{-2\eta})(e^{\mp(q+1)\eta}-\lambda^b)}{1-\lambda^2}\right]=1 \ , \tag{5.11}$$

which is satisfied by taking

$$\lambda=e^\eta, \quad A_\pm=-e^{\pm q\eta} \ . \tag{5.12}$$

Similarly, substituting Eq. (4.23) with $\epsilon_a=-1$ in Eqs. (5.2a) and (5.3a) required by Reidemeister moves IIA and IIB, we verify that they are also satisfied with the choice of Eq. (5.12). For example, to verify Eq. (5.2a), which is the same as the unitarity relation Eq. (4.8), one substitutes Eq. (5.12), which equates the left-hand side of Eq. (5.2a) to

$$\begin{aligned}\text{LHS}=\sum_{b,y\in\mathcal{J}}&[-e^{-\eta}\delta_{abxy}+(\delta_{ab}\delta_{xy}-\delta_{abxy})+(e^\eta-e^{-\eta})\theta(b-a)\delta_{ay}\delta_{bx}]\\ &\times[-e^{\eta}\delta_{yzbc}+(\delta_{ba}\delta_{yz}-\delta_{bcyz})=(e^\eta-e^{-\eta})\theta(y-z)\delta_{yc}\delta_{bz}] \ .\end{aligned} \tag{5.13}$$

Expanding the fist square bracket in Eq. (5.13) and carrying out the summations term by term, one obtains

$$\begin{aligned}\text{LHS}&=-e^{-\eta}[(-e^{\eta}\delta_{acxz})+0+0]+[0+(\delta_{ac}\delta_{xz}-\delta_{acxz})+0]+(e^\eta-e^{-\eta})[0+0+0]\\ &=\delta_{ac}\delta_{xz} \ .\end{aligned} \tag{5.14}$$

This establishes Eq. (5.2a). In a similar fashion and using Eq. (5.10) in conjunction with the identity

$$\sum_{b\in\mathcal{J}}\theta(a-b)\theta(b-c)\lambda^b=(\lambda^{c+2}-\lambda^a)/(1-\lambda^2) \ , \tag{5.15}$$

we verify that Eq. (5.3a) is satisfied. It can also be checked, although this is not necessary, that the condition (5.4) required by Reidemeister moves IIIB is also satisfied.

Combining Eqs. (5.12) with (4.17b) and (4.23), we arrive at the following explicit expression for the angle-dependent vertex weight:

$$\omega_\pm^*\begin{bmatrix}c & d\\ a & b\end{bmatrix}=e^{\pm q\eta}((e^{\pm\eta}+1)\delta_{abcd}-\delta_{ad}\delta_{bc}\mp(e^\eta-e^{-\eta})e^{(a-d)\eta\theta/2\pi}\theta[\pm(b-a)]\delta_{ac}\delta_{bd}) \ . \tag{5.16}$$

Here θ is the angle between the two incoming arrows at the vertex, and $\theta(a)$ is the step function defined by Eq. (4.24). The partition function $Z(\omega_\pm^*)$ of this vertex model generates knot invariant.[15]

To see that this knot invariant is the Homfly polynomial, we need to establish the Skein relation (5.6). Indeed, using the identity

$$\theta(a-b)+\theta(b-a)+\delta_{ab}=1 \ , \tag{5.17}$$

one verifies that Eq. (5.6) is satisfied by the $\omega_\pm^*$ Eq. (5.16) by identifying

$$t=e^{q\eta}, \quad z=e^{-\eta}-e^{\eta} \ . \tag{5.18}$$

Furthermore, as discussed in Sec. II.C.1, the Skein relation expresses the partition function $Z(q,e^\eta)$ of the enhanced spin-conserving vertex model as the product of

[14]The choice of $\epsilon_a=1$, which leads to $\lambda=e^{-\eta}$ and $A_\pm=e^{\mp q\eta}$, also yields the Homfly polynomial.

[15]It is instructive to verify that the vertex weight (5.16) does not disentangle the configurations shown in Fig. 8. Thus the vertex weight (5.16) is exactly what is required of knot invariances, no more and no less.

two factors: a Laurent polynomial $P(t,z)$ in t and z and the partition function of a ring, $Z_{\text{ring}}=\sinh q\eta/\sinh\eta$, deduced from Eq. (4.12). Thus the Laurent polynomial

$$P(t,z)=\left[\frac{\sinh\eta}{\sinh q\eta}\right]Z_{\text{vertex}}(q,e^{\eta}) \tag{5.19}$$

satisfies the normalization condition (2.9) and hence is the Homfly polynomial for integral q. By analytically continuing Eq. (5.19) to all values of q, we establish the existence and uniqueness of the Homfly polynomial $P(t,z)$ for general t and z. This completes the construction of the Homfly polynomial.

3. The Jones polynomial

We have seen in Sec. II.D.3 that the Jones polynomial $V(t)$ is obtained from the Homfly polynomial $P(t,z)$ by taking $z=\sqrt{t}-1/\sqrt{t}$, indicating that the Jones polynomial is constructed from the $q=2$ spin-conserving vertex model. In view of its fundamental importance, we give here another construction of the Jones polynomial using the nonintersecting-string model of Sec. IV.E.3 (Lipson, 1992; Wu, 1992b). This construction is direct, as there is no need of introducing piecewise-linear lattices nor the writhe; it also expresses the Jones polynomial directly as a Potts model partition function (Wu, 1992b).

In the nonintersecting-string model we have $\lambda=1$, so that there is no angle dependence in vertex weights. As before, the condition for Reidemeister moves IIIA is automatically satisfied by the vertex weight (4.36). Substituting this weight in Eq. (5.1a) with $\lambda=1$, we obtain

$$A_{\pm}=-e^{\pm 2\eta},\quad q=e^{\eta}+e^{-\eta}\ . \tag{5.20}$$

Explicitly, the vertex weight Eq. (4.36) is now

$$\omega_{\pm}\begin{bmatrix} c & d\\ a & b\end{bmatrix}=-e^{\pm 2\eta}\delta_{ab}\delta_{cd}+e^{\pm\eta}\delta_{ac}\delta_{bd}\ . \tag{5.21}$$

It can be checked that Eqs. (5.2a) and (5.3a) are now satisfied by Eq. (5.21). Hence, the partition function $Z(q,e^{\eta})$ of the nonintersecting-string model with weight (5.21) is a knot invariant. To identify this knot invariant as the Jones polynomial, we obtain from Eq. (5.21)

$$e^{-2\eta}\omega_{+}^{*}\begin{bmatrix} c & d\\ a & b\end{bmatrix}-e^{2\eta}\omega_{-}^{*}\begin{bmatrix} c & d\\ a & b\end{bmatrix}$$

$$=(-e^{\eta}+e^{-\eta})e^{(a-d)\theta/2\pi}\delta_{ac}\delta_{bd}\ . \tag{5.22}$$

This leads to the Skein relation Eq. (2.6) for $V(t)$ upon identifying $e^{\eta}=-\sqrt{t}$. Furthermore, $Z(q,e^{\eta})$ is proportional to $Z_{\text{ring}}(q,e^{\eta})=q$. It follows that the Laurent polynomial

$$V(t)=q^{-1}Z_{\text{vertex}}(q,e^{\eta}) \tag{5.23}$$

is the Jones polynomial when one sets

$$q=-(\sqrt{t}+1/\sqrt{t}),\quad e^{\eta}=-\sqrt{t}\ . \tag{5.24}$$

Another construction of the Jones polynomial based on the nonintersecting-string model will be given in Sec. V.B.2 below.

4. The Alexander-Conway polynomial

The Alexander-Conway polynomial $\nabla(z)$ is obtained from the Homfly polynomial $P(t,z)$ by taking $t=1$. According to Eq. (5.18), this corresponds to taking $q=0$ in our derivation of $P(t,z)$. We shall therefore assume that we have analytically continued Eq. (5.19) to permit us to take the $q\to 0$ limit. This is very much similar to the $q\to 0$ limit of the Potts model, which generates percolations (Fortuin and Kasteleyn, 1972).

Alternatively, $\nabla(z)$ can also be constructed from a two-state vertex model (Kauffman, 1991). This is done by considering two-strand knots which convert to lattices possessing two open lattice edges. It can then be shown that the partition function of a $q=2$ spin-conserving vertex model with weights given by Eqs. (4.23) and (4.17b), with $q=2$, $\{a,b,c,d\}=\pm 1$, $\epsilon_{\pm 1}=\pm 1$, and $\lambda=\sqrt{-1}$, gives rise to $\nabla(e^{\eta}-e^{-\eta})$ for two-strand knots. Readers are referred to Kauffman (1991) for details of this analysis.

5. The Akutsu-Wadati polynomial

In a similar fashion the angle-dependent vertex weight (4.17b) with $\lambda=e^{2\eta}$ and $\omega_{\pm}$ given by Eqs. (4.29)–(4.31) for the N-state vertex model can be used to derive knot invariants. This leads to the Akutsu-Wadati polynomial $A^{(N)}(t)$ (Akutsu and Wadati, 1987a, 1987b). Expressions for the $N=3$ Akutsu-Wadati polynomial have been obtained, and tabulated, for knots of closed three-braids (Akutsu *et al.*, 1987). The extension to two-variable polynomials has been made (Deguchi *et al.*, 1988), and Ge *et al.* (1989) have also given an explicit derivation of the $N=3,4$ polynomials. The Akutsu-Wadati polynomial satisfies the general Skein relation relating knots with configurations L_{-}, L_{0}, L_{+}, and L_{n+}, $n=2,3,\ldots,N-1$, and is more powerful than the Jones polynomial in differentiating knots. For example, the two knots found by Birman (1985) to possess an identical Jones polynomial can be distinguished using the Akutsu-Wadati polynomial (Akutsu *et al.*, 1987).

B. Unoriented knots

1. Formulation

Polynomial invariants for unoriented knots can be constructed by following the same route as that for oriented knots. For each knot one constructs an *unoriented* lattice $\mathcal{L}$. Consider a vertex model on $\mathcal{L}$ and require the partition function to remain invariant under all Reidemeister moves of lattice edges. The partition function is then a knot invariant.

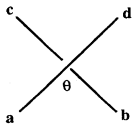

FIG. 32. Labelings of a vertex for unoriented knots.

For unoriented knots, however, there is only one type of line crossing, and hence the partition function has a uniform vertex weight. We label the vertex edges as in Fig. 32 and write the vertex weight as

$$\omega(a,d|b,c)=\omega\begin{bmatrix} c & d \\ a & b \end{bmatrix}=\omega\begin{bmatrix} b & a \\ d & c \end{bmatrix} . \tag{5.25}$$

If we further label the Reidemeister moves as shown in Fig. 33, assuming regular isotopy and Eq. (2.15) for type-I moves, we can read off from Fig. 33 conditions imposed by Reidemeister moves. This leads to

$$\sum_{c\in\mathcal{J}} \omega(a,c|b,c)=\alpha^{-1}\delta_{bx} , \tag{5.26a}$$

$$\sum_{c\in\mathcal{J}} \omega(c,b|a,c)=\alpha\delta_{ab} , \tag{5.26b}$$

$$\sum_{b,y\in\mathcal{J}} \omega(a,b|x,y)\omega(b,c|y,z)=\delta_{ac}\delta_{xz} , \tag{5.26c}$$

$$\sum_{xyz\in\mathcal{J}} \omega(x,b|y,a)\omega(f,z|e,x)\omega(z,c|d,y) = \sum_{xyz\in\mathcal{J}} \omega(e,x|d,y)\omega(z,c|x,b)\omega(f,z|y,a) , \tag{5.26d}$$

where, as before, $\mathcal{J}$ is a set of q integers. We now state the main result as a theorem:

Theorem V.B.1. For a given knot we construct an unoriented lattice $\mathcal{L}$. The partition function $Z(\omega)$ [Eq. (4.1)] of a vertex model on $\mathcal{L}$ with vertex weight as given in Eq. (5.25) and satisfying Eq. (2.15) under type-I Reidemeister moves is an invariant of regular isotopy for unoriented knots, provided that Eqs. (5.26a)–(5.26d) hold.

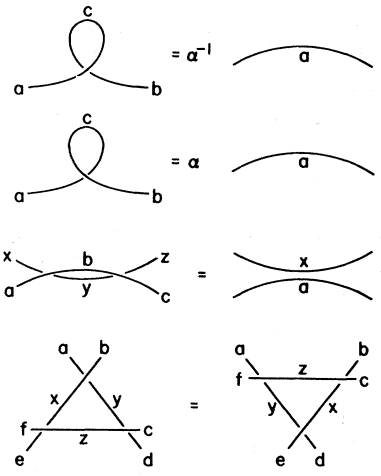

FIG. 33. Labelings for Reidemeister moves.

Collorary V.B.1. The function $\alpha^{-w(K)}Z(\omega)$ is a semioriented invariant for oriented knots.

2. The bracket polynomial and ice-type vertex models

As an example, we construct an invariant using the nonintersecting-string model of Sec. IV.E.3, which leads to the Jones polynomial.

For the vertex shown in Fig. 32, we assign the vertex weight given by Eqs. (4.33) and (4.35), namely,

$$\omega\begin{bmatrix} c & d \\ a & b \end{bmatrix}=A\delta_{ac}\delta_{bd}+B\delta_{ab}\delta_{cd} , \tag{5.27}$$

where $A\equiv\sinh(\eta-u)$, $B\equiv\sinh u$. Note, however, that we regard A and B as two independent parameters and apply the vertex weight (5.27) to all vertices.

Perk and Wu (1986a) pointed out that the particular form of the weight given in Eq. (5.27) permits one to write the partition function $Z_{\rm NIS}$ as a generating function of nonintersecting polygonal decompositions P of $\mathcal{L}$. Indeed, by substituting Eq. (5.27) into Eq. (4.1) and summing over all edge states, one finds $Z_{\rm NIS}$ in the form of a polynomial in q, A, and B (Perk and Wu, 1986a),

$$Z_{\rm NIS}(q,A,B)=\sum_P q^{p(P)}\prod_{i=1}^{N} W_i(P) , \tag{5.28}$$

where $p(P)$ is the number of polygons (loops) in P, and $W_i(P)$ is the weight of the ith site in P, equal to either A or B. Since the lattice has at least one loop, $Z_{\rm NIS}$ is divisible by q.

The polynomial

$$P(q,A,B)=q^{-1}Z_{\rm NIS}(q,A,B) \tag{5.29}$$

was discovered independently by Kauffman and named the *bracket polynomial* of a *state model* (Kauffman, 1987a). Clearly, in this picture, the state model is characterized by *nonlocal* Boltzmann weights. In a remarkable piece of pioneering insight connecting knot theory with statistical mechanics, Kauffman (1987a) showed that the bracket polynomial can be used to provide a simple derivation of the Jones polynomial (see also Wu, 1992a). Perk and Wu (1986a), Truong (1986), and Kauffman (1988b) have also shown that the bracket polynomial is completely equivalent to a q^2-state Potts model partition function, a fundamental connection relating the Potts model with the Jones polynomial. Kauffman (1988b) went further and reformulated the Potts model in terms of a formalism of alternating link diagrams.

It is straightforward to verify that Eqs. (5.26a)–(5.26d) are satisfied by taking

$$B=A^{-1},\quad q=-(A^2+A^{-2}),\quad \alpha=-A^3 . \tag{5.30}$$

It follows from Theorem V.B.1 that the one-variable function

$$f(A)=P(-A^2-A^{-2},A,A^{-1}) , \tag{5.31}$$

which is normalized to $f_{\text{ring}}(A)=1$, is an invariant for unoriented knots. This is the Kauffman bracket invariant. Furthermore, by Corollary V.B.1, the function

$$V(t)=(-t^{-3/4})^{-w}f(t^{-1/4}) \tag{5.32}$$

is an invariant of ambient isotopy for oriented knots, where we have written $A=t^{-1/4}$. To identify $V(t)$ as the Jones polynomial, one verifies the identity

$$\frac{1}{t}\left[\alpha^{-1}\omega\begin{bmatrix}c & d\\ a & b\end{bmatrix}\right]-t\left[\alpha\omega\begin{bmatrix}d & b\\ c & a\end{bmatrix}\right] = \left[\sqrt{t}-\frac{1}{\sqrt{t}}\right]\delta_{ac}\delta_{bd} . \tag{5.33}$$

This shows that $V(t)$ satisfies the Skein relation (2.6) and hence is the Jones polynomial.

The noninteracting-string model can be further generalized by associating line orientations. This leads to the oriented nonintersecting-string (ONIS) and generalized ice-type models (Perk and Wu, 1986a). In the ONIS model the lattice edges can be colored in q_1 distinct colors and, in addition, colored as well as oriented in q_2 colors, with the restriction that the numbers of in and out arrows of a given color at a vertex must be the same (the ice rule). This permits one to consider the piecewise-linear lattice $\mathcal{L}^*$ and introduce, for vertices of degree 2, weights in the form of Eq. (4.9) with λ_μ, $\mu=1,2,\ldots,q_2$ replacing λ for each of the q_2 colors. For a model with separable weights one finds the partition function again given by Eq. (5.28), but with

$$q=q_1+\sum_{\mu=1}^{q_2}(\lambda_\mu+\lambda_\mu^{-1}) . \tag{5.34}$$

The case of $q_1=0$, $q_2=1$ leads to the usual ice-rule model (Temperley and Lieb, 1971; Baxter *et al.*, 1976), a correspondence that has also been discussed by Kauffman (1988b).

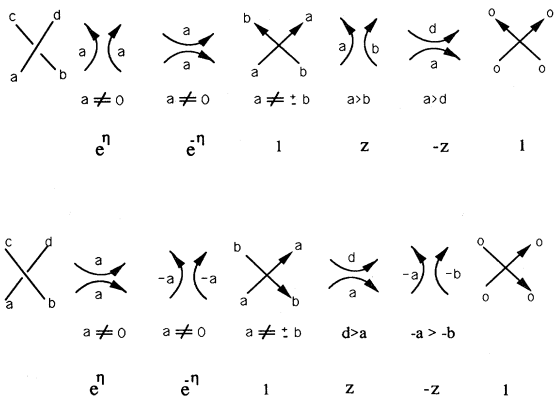

FIG. 34. Vertex configurations and weights for the Kauffman polynomial. Configurations in the two rows are related by a 90° rotation.

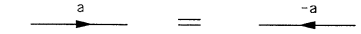

FIG. 35. Orientation and sign convention.

3. The Kauffman polynomial

The construction of the Kauffman polynomial (Turaev, 1988) requires special attention. The following is essentially a reformulation of the diagrammatic analysis (of the Turaev construction) due to Kauffman (1991), modified by considering a vertex model with local weights on piecewise-linear lattices.

To begin with consider a $(q+1)$-state vertex model with edge variables $\{a,b,\ldots,x,y,\ldots\}$ taking on $q+1$ numerical values contained in the set

$$\mathcal{I}_P=\{\mathcal{I},0\} , \tag{5.35}$$

Here $\mathcal{I}$ is the set of q numerical values given by Eq. (5.8). For our purposes we shall consider $q=2,4,6,\ldots$ so that $\mathcal{I}$ does not contain the value zero.[16]

Again, one looks for vertex weights that are solutions of the Yang-Baxter equation (5.26d), so that the Reidemeister move III is automatically satisfied. To obtain the Kauffman polynomial one uses a representation of simple Lie algebras $A_{q-1}^{(1)}$, giving rise to nonvanishing vertex weights of the form (Turaev, 1988)

$$\omega\begin{bmatrix}a & b\\ a & b\end{bmatrix},\quad \omega\begin{bmatrix}b & -b\\ a & -a\end{bmatrix},\quad \text{or } \omega\begin{bmatrix}a & b\\ b & a\end{bmatrix} . \tag{5.36}$$

However, to write down the explicit expression of ω we need first to orient and decompose $\mathcal{L}$.

Connect at each vertex the edge indexed a with that indexed $\pm a$, and b with $\pm b$, a process that is unique and that leads to one of the six configurations shown in the first row of Fig. 34. This process decomposes $\mathcal{L}$ into disconnected components, each of which contains an edge in states $\pm a$. [Components may cross each other via bridges, however, due to the presence of the third vertex weight in Eqs. (5.36) and (5.37).] To uniquely specify each component by a single index, we now *orient* components and adopt the convention that

(i) the negation of an edge variable has the same effect as reversing the orientation, a situation shown in Fig. 35, and

(ii) a component has the same index as its upward-pointing edges at the vertex shown in Fig. 32, assuming the latter vertex edges are oriented to point upward.

Thus configurations that can occur at a vertex are those shown in the first row of Fig. 34 with weights

[16]For $q=$odd the construction of the Kauffman polynomial still holds, but there are then two zeros in the set $\mathcal{I}_P$, and one needs to distinguish them carefully in Eq. (5.37) and Fig. 34 below.

$$\omega\begin{bmatrix} a & a \\ a & a \end{bmatrix}=e^{\eta},\quad a\neq 0\ ,$$

$$\omega\begin{bmatrix} -a & a \\ a & -a \end{bmatrix}=e^{-\eta},\quad a\neq 0\ ,$$

$$\omega\begin{bmatrix} b & a \\ a & b \end{bmatrix}=1,\quad a\neq\pm b\ ,$$

$$\omega\begin{bmatrix} a & b \\ a & b \end{bmatrix}=z,\quad a>b\ , \tag{5.37}$$

$$\omega\begin{bmatrix} -d & d \\ a & -a \end{bmatrix}=-z,\quad a>d\ ,$$

$$\omega\begin{bmatrix} 0 & 0 \\ 0 & 0 \end{bmatrix}=1\ ,$$

$$\omega\begin{bmatrix} c & d \\ a & b \end{bmatrix}=0,\quad \text{otherwise}\ ,$$

where η is arbitrary and

$$z=e^{\eta}-e^{-\eta}\ . \tag{5.38}$$

Note that edges with state zero also form connected components. For later use we show in the second row of Fig. 34 the same configurations rotated 90° clockwise, where we have adopted the sign and orientation convention and negated some edge variables.

The weight equation (5.37) can be summarized as

$$\begin{aligned}\omega\begin{bmatrix} c & d \\ a & b \end{bmatrix}&=e^{\eta}\delta_{abcd}(1-\delta_{a0})+e^{-\eta}\delta_{a,-b-c,d}(1-\delta_{a0})\\&\quad+\delta_{ad}\delta_{bc}(1-\delta_{ab})(1-\delta_{a,-b})+z\delta_{ac}\delta_{bd}\theta(a-b)\\&\quad-z\delta_{b,-a}\delta_{c,-d}\theta(a-d)+\delta_{abcd0}\\&=\omega\begin{bmatrix} -b & -a \\ -d & -c \end{bmatrix}\ .\end{aligned} \tag{5.39}$$

Note that the symmetry of the vertex weight indicated in the last line is different from that given in Eq. (5.25). However, due to the sign and orientation convention, the symmetry shown ensures its consistency and does not affect the overall partition function.

Substituting Eq. (5.39) into the partition function equations (4.1) and (4.2), we can write the partition function as

$$Z_{\text{vertex}}(\omega)=\sum_{a\in c}\sum_{i}\omega_i\ , \tag{5.40}$$

where the summation is taken over all possible decompositions of $\mathcal{L}$ into oriented components c, each of which is now indexed by a single edge variable a.

We next introduce the piecewise-linear lattice $\mathcal{L}^*$ with angle-dependent vertex weights. For vertices of degree two, the weights $\omega^*(a)$ are those given previously in Eq. (4.9). For other vertices, we require that the new weight ω^* satisfy the Yang-Baxter equation. If we color components of $\mathcal{L}$ by different colors, then as seen in Fig. 34 the incoming/outgoing colors are conserved at each vertex. This color conservation, which is a special case of charge conservation in the sense that charges (colors) remain unchanged, permits us to introduce angle factors as in Eq. (4.17b) for each term in Eq. (5.39), leading to the new weight

$$\begin{aligned}\omega^*\begin{bmatrix} c & d \\ a & b \end{bmatrix}(\theta)&=e^{\eta}\delta_{abcd}(1-\delta_{a0})+e^{-\eta}\delta_{a,-b,-c,d}(1-\delta_{a0})+\delta_{ad}\delta_{bc}(1-\delta_{ab})(1-\delta_{a,-b})+z\lambda^{(a-d)\theta/2\pi}\delta_{ac}\delta_{bd}\theta(a-d)\\&\quad-z\lambda^{(d-a)(\pi-\theta)/2\pi}\delta_{a,-b}\delta_{c,-d}\theta(a-d)+\delta_{abcd0}\\&=\omega^*\begin{bmatrix} -b & -a \\ -d & -c \end{bmatrix}\ .\end{aligned} \tag{5.41}$$

As a consequence of color conservation, the weight ω^* now satisfies the Yang-Baxter equation.[17] The partition function $Z(\omega^*)$ with angle-dependent weights is now invariant under Reidemeister moves IIIA of the lattice edges.

The expression of ω^* differs from that of ω only in the appearance of angle-dependent factors in the fourth and fifth terms. In the latter (fifth) term we can write $\lambda^{(d-a)(\pi-\theta)/2\pi}=\lambda^{(d-a)/2}\lambda^{(a-d)\theta/2\pi}$, giving rise to a factor $\lambda^{(a-d)/2}$ noted in another context (Kauffman, 1991). Here this factor arises naturally as a consequence of the requirement that ω^* satisfy the Yang-Baxter equation.

We now choose λ so that $Z(\omega^*)$ is invariant under the two distinct Reidemeister moves I shown in Fig. 36. Adopting line orientations as shown, we obtain from Eq. (2.15) the conditions

[17]This fact can also be seen by noting that ω^* can be generated from ω by separating the angle-dependent factor into factors $\lambda^{\pm a\theta/2\pi}$ and associating them separately with the two paths of different colors passing through a vertex. The desired property can then be established by using the property Eq. (4.10).

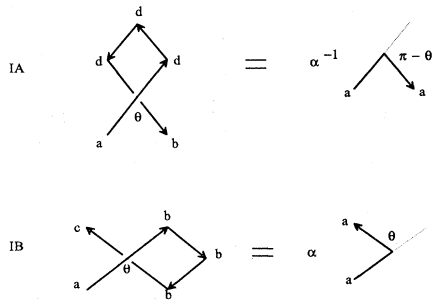

FIG. 36. Labelings for Reidemeister moves I.

$$\sum_{d\in\mathcal{J}_P}\lambda^{d(\pi+\theta)/2\pi}\omega^*\begin{bmatrix}-d & d\\ a & -b\end{bmatrix}(\theta)$$

$$=\alpha^{-1}\lambda^{-a(\pi-\theta)/2\pi}\delta_{a,-b}\quad\text{(IA)}\,,\qquad(5.42)$$

$$\sum_{b\in\mathcal{J}_P}\lambda^{-b(2\pi-\theta)/2\pi}\omega^*\begin{bmatrix}c & b\\ a & b\end{bmatrix}(\theta)=\alpha\lambda^{a\theta/2\pi}\delta_{ac}\quad\text{(IB)}\,,$$

(5.43)

where, as in Eq. (5.1), we have included weights of the three vertices of degree 2.

When we substitute Eq. (5.41) into Eq. (5.43) and use the identity

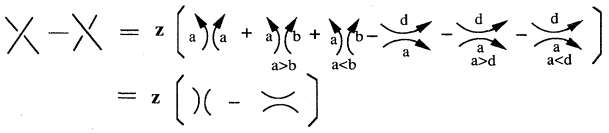

FIG. 37. Skein relation for the Kauffman polynomial.

$$\sum_{d\in\mathcal{J}_P}\lambda^{-d}\theta(a-d)=(1-\delta_{a0})\theta(a)+\left[\frac{\lambda^{q-1}-\lambda^{-a}}{1-\lambda^{-2}}\right]+\left[\frac{1-\lambda^{-1}}{1-\lambda^{-2}}\right]\delta_{a0}\,,$$

(5.44)

it is straightforward to show that Eq. (5.43) is satisfied if we take

$$\lambda=e^{\eta},\quad\alpha=e^{-q\eta}\,.\qquad(5.45)$$

In a similar manner one shows that Eq. (5.42) is satisfied. One also establishes that conditions imposed by Reidemeister moves II (and III) are all satisfied by the vertex weight (5.41), details of which we omit. It follows that the partition function $Z(\omega^*)$ defines a knot invariant.

To identify this knot invariant as the Kauffman polynomial, we need to show that the partition function $Z(\omega^*)$ satisfies the Skein relation (2.13) or (2.13a). Now the vertex configurations and weights of a minus-type crossing are given in the second row in Fig. 34 (for which the "upward-pointing" direction is pointing towards the right). By taking the difference of the two weights in Fig. 34 and making use of the identity (5.17), one obtains

$$\omega^*\begin{bmatrix}c & d\\ a & b\end{bmatrix}(\theta)=\omega^*\begin{bmatrix}d & -b\\ -c & a\end{bmatrix}(\pi-\theta)=z[\lambda^{(a-d)\theta/2\pi}\delta_{ac}\delta_{bd}-\lambda^{(d-a)(\pi-\theta)/2\pi}\delta_{a,-b}\delta_{c,-d}]\,.\qquad(5.46)$$

Here the negation of b and c in the second expression in Eq. (5.46) is due to our orientation convention.

Inserting this expression into $Z(\omega^*)$ written in the form of Eq. (5.40), a procedure shown schematically in Fig. 37, one arrives at the identity

$$Z_{D_+}(\omega^*)-Z_{D_-}(\omega^*)=z[Z_{D_0}(\omega^*)-Z_{D_\infty}(\omega^*)]\,,\qquad(5.47)$$

which is precisely the Skein relation (2.13a) for the Dubrovnik version of the Kauffman polynomial.

As before, recursive applications of the Skein relation eventually equate $Z(\omega^*)$ to the product of two factors, a Laurent polynomial in α and z, and the partition function of a ring, now given by

$$Z_{\rm ring}(\alpha,z)=\sum_{a\in\mathcal{J}_P}\lambda^{\pm a}=1+\frac{\sinh q\eta}{\sinh\eta}$$

$$=1+(\alpha-\alpha^{-1})/z\,.\qquad(5.48)$$

It follows that the Laurent polynomial

$$Q(\alpha,z)=Z_{\rm vertex}(\omega^*)/Z_{\rm ring}(\alpha,z)\,,\qquad(5.49)$$

normalized to $Q_{\rm unknot}(\alpha,z)=1$, is the Dubrovnik version of the Kauffman polynomial. By analytically continuing $Z_{\rm vertex}(e^{q\eta},e^{\eta}-e^{-\eta})$ to all q, we finally establish the existence and uniqueness of $Q(\alpha,z)$ for arbitrary α and z. This completes the construction of the Kauffman polynomial.

VI. KNOT INVARIANTS FROM IRF MODELS

A. The IRF model

Consider a directed lattice $\mathcal{L}$ of N sites, arbitrary shape, and a uniform coordination number 4. Place spins inside the faces of $\mathcal{L}$ as shown in Fig. 38, where the spin locations are indicated by solid circles. Let the spins take on values, or spin states, designated by variables $\{a,b,\ldots\}\in\mathcal{J}$, where $\mathcal{J}$ is a set of q integers. Let the

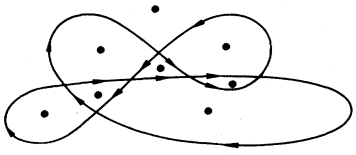

FIG. 38. A directed lattice for the interaction-round-a-face (IRF) model. Spins are denoted by solid circles.

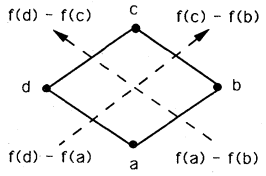

FIG. 39. The four interacting spins in the IRF model. Edge indices are defined as in Fig. 42.

four spins surrounding a site of $\mathcal{L}$ interact via a Boltzmann weight $B(a,b,c,d)$, where spins a, b, c, d are arranged as shown in Fig. 39. In the figure we have drawn the edges of $\mathcal{L}$ as broken lines and connected the four spins along the edges of $\mathcal{L}_D$, the dual of $\mathcal{L}$, to indicate the "domain" of the interaction.

If one regards spin states $a,b,\ldots$ as defining heights, then an overall spin configuration describes a height assignment of faces of $\mathcal{L}$. This is then a solid-on-solid (SOS) model describing the interface of two solids. The overall Boltzmann factor W is a product of individual Boltzmann weights B, and the partition function (3.1) reads

$$Z_{\rm IRF}(B)=\sum_{\{\rm heights\}}\prod_{i=1}^{N}B_i(a,b,c,d)\ . \tag{6.1}$$

Here the product is taken over all vertices of $\mathcal{L}$ or, equivalently, all faces $\mathcal{L}_D$, including the exterior (infinite) one. This defines an interaction-round-a-face (IRF) model (Baxter, 1980).

Generally there can be q^4 different Boltzmann weights $B(a,b,c,d)$. But in practice one considers IRF models for which $B(a,b,c,d)$ vanishes unless the heights of two neighboring (adjacent) faces are related in a specific way. For example, the *restricted* eight-vertex SOS model solved by Andrews, Baxter, and Forrester (1984), the ABF model, is an SOS model with *q finite* and for which the difference of two adjacent heights is always 1. Particularly, the $q=\infty$ version is the *unrestricted* eight-vertex SOS model. Such rules are conveniently represented by line graphs in which heights are represented by numbered dots and allowed adjacent heights by line connections.[18] For example, the unrestricted eight-vertex SOS model is described by the graph shown in Fig. 40, and the ABF model is described by graph A_q in Fig. 41.

Generally, there is a one-to-one correspondence between line graphs and certain IRF models (Akutsu *et al.*, 1988), a consideration leading to hierarchies of integrable models (Date *et al.*, 1986; see also Akutsu *et al.*, 1986a, 1986b; Kuniba *et al.*, 1986a–1986e; Pearce and Seaton, 1988). In particular, there exists an integrable IRF mole for each Dynkin diagram of simply-laced classical or affine Lie algebras of the A, D, E series (Pasquier, 1987a; Jimbo *et al.*, 1988), examples of which are shown in Fig. 41. The IRF model corresponding to A_n is the ABF model; the model corresponding to D_n has been solved by Pasquier (1987b), and the cyclic eight-vertex SOS model (Baxter, 1973a, 1973b) corresponding to $A_n^{(1)}$ has been solved by Pearce and Seaton (1989).

B. Equivalence with charge-conserving vertex models

The construction of knot invariants from IRF models is most conveniently done via the equivalence of IRF models with a charge-conserving vertex model. We first elucidate this equivalence (Akutsu *et al.*, 1988; Jones, 1989; see also Kadanoff and Wegner, 1971 and Wu, 1971).

Consider an IRF model with the partition function (6.1). Consider further the partition function $Z_{\rm IRF}^{(a)}(B)$ defined by Eq. (6.1) with the height of one face, say, the exterior, fixed at a. Then Eq. (6.1) can be written as

$$Z_{\rm IRF}(B)=\sum_{a\in\mathcal{J}}Z_{\rm IRF}^{(a)}(B)\ . \tag{6.2}$$

To each height a we assign a value $f(a)$ where the function f is one-to-one; to each directed edge we assign an index

$$h_{ab}=f(a)-f(b)\ , \tag{6.3}$$

where a is the height to the left, and b to the right, of the edge, as shown in Fig. 42. An example of f is $f(a)=a$; but more generally the function f can be chosen at our discretion. A height configuration is now mapped into an edge indexing. Clearly, as can be seen from Fig. 39, the edge indexing satisfies the charge conservation condition, Eq. (4.16), as generalized in footnote 9. Conversely, each charge-conserving edge indexing in the form of Eq. (6.3) is mapped into a height configuration, provided that the height a, or the function $f(a)$, of the exterior face is given. This leads to the equivalence

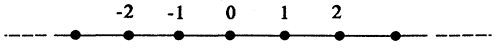

FIG. 40. Line graph for the Andrews, Baxter, and Forrester (ABF) model.

[18]The connecting lines will be directed in the case of IRF models with chiral Boltzmann weights.

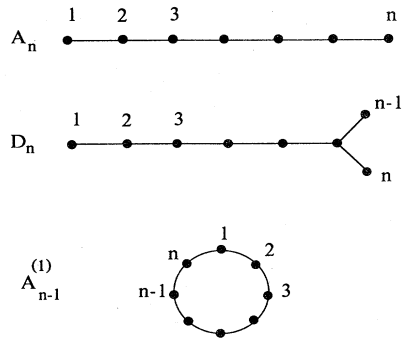

FIG. 41. Dynkin diagrams of Lie algebras.

$$Z^{(a)}_{\rm IRF}(B)=Z^{f(a)}_{\rm vertex}(w)\ , \tag{6.4}$$

where $Z^{f(a)}_{\rm vertex}(w)$ is the vertex-model partition function (4.1), with edges indexed by h_{ab}, and the function f of the exterior face fixed at $f(a)$. Explicitly, we have the equivalence

$$\omega\begin{bmatrix} f(d)-f(c) & f(c)-f(b) \\ f(d)-f(a) & f(a)-f(b)\end{bmatrix}=B(a,b,c,d)\ . \tag{6.5}$$

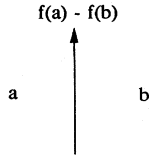

FIG. 42. Convention of lattice edge indexing.

C. The Yang-Baxter equation

An IRF model is *integrable* if its Boltzmann weight $B(a,b,c,d)$ satisfies a Yang-Baxter equation. The Yang-Baxter equation can now be written down from the equivalence with a vertex model, by assuming appropriate edge indexings in Eqs. (4.3) and (4.4). To completely describe the Yang-Baxter equation, one needs further to specify the factor $f(a)$ associated with the exterior face. It is then more convenient to write down the Yang-Baxter equation directly in terms of the IRF-model Boltzmann weights $B(a,b,c,d)$. As may be surmised from Fig. 43, this is equivalent to considering a cluster of seven spins with interactions arranged in two different ways, as shown, and requiring the partition functions of the two clusters to be identical for any given spin states $\{a,b,c,d,e,f\}$. The Yang-Baxter equation in IRF language then reads (Baxter, 1980)

$$\sum_{g\in\mathcal{J}} B(g,c,b,a|u-w)B(f,e,g,a|v-u)B(e,d,c,g|v-w)$$
$$=\sum_{g\in\mathcal{J}} B(e,d,g,f|u-w)B(g,d,c,b|v-w)B(f,g,b,a|v-w)\ \text{ for all } a,b,c,d,e,f\in\mathcal{J}\ . \tag{6.6}$$

The unitarity condition, Eq. (4.5b), now reads, after changing edge indexings,

$$\sum_{c\in\mathcal{J}} B(a,b,c,d|u-v)B(c,b,d,e|v-u)=\delta_{ae}\ , \tag{6.7}$$

which we show graphically in Fig. 44. In analogy to Eq. (4.18) for the vertex model, one verifies that the Boltzmann weight

$$\tilde{B}(a,b,c,d|u)=e^{\beta(f_a+f_c-f_b-f_d)u}B(a,b,c,d|u) \tag{6.8}$$

is also a solution of Eq. (6.6) for any β. We shall leave open, the possibility of using this symmetry-breaking Boltzmann weight, and use B to denote either B or $\tilde{B}$, whichever arises in applications. In the infinite-rapidity limit, we have

$$B_{\pm}(a,b,c,d)=\lim_{u\to\pm\infty} B(a,b,c,d|u)\ , \tag{6.9}$$

where, as before, the right-hand side of Eq. (6.9) has been divided by the leading diverging Boltzmann weight.

D. Integrable IRF models

We now present examples of integrable IRF models.

1. The unrestricted eight-vertex SOS model

The unrestricted eight-vertex SOS model, the $q=\infty$ ABF model, is characterized by the line graph of Fig. 40.

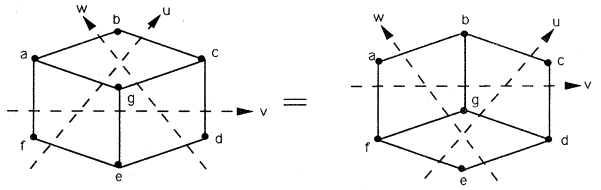

FIG. 43. The Yang-Baxter equation for IRF models.

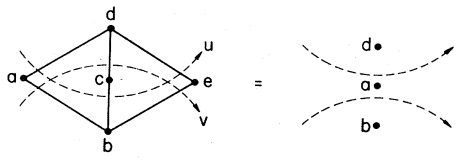

FIG. 44. The unitarity condition for Boltzmann weights.

In this model, adjacent heights always differ by 1, and there are six contributing configurations, as shown in Fig. 45. It is also clear that we need only consider the partition function $Z^{(a)}(B)$.

Boltzmann weights of integrable IRF models are given in terms of elliptical theta functions. At criticality, however, they reduce to hyperbolic functions. In the case of the $q=\infty$ ABF model they can be written in the form

$$\begin{aligned} B_1&=B_2=1\ ,\\ B_3&=B_4=\sinh u/\sinh(\eta-u)\ .\\ B_5&=e^{u}\sinh\eta/\sinh(\eta-u)\ ,\\ B_6&=e^{-u}\sinh\eta/\sinh(\eta-u)\ , \end{aligned} \tag{6.10}$$

where u is the rapidity and η is arbitrary, and we have included the symmetry-breaking factor in Eq. (6.8) with $\beta=1/2$ and $f(a)=a$.

The Boltzmann weights of Eq. (6.10) can be rewritten as

$$\begin{aligned} &B(a,b,c,d|u)\\ &\quad=\delta_{ac}+\delta_{bd}\left[\frac{\sinh u}{\sinh(\eta-u)}\right]e^{[(a+c)/2-b]\eta}\\ &\quad=0,\quad (a-b)(b-c)(c-d)(a-d)\neq\pm1\ , \end{aligned} \tag{6.11}$$

where a,b,c,d are integers. Taking the infinite-rapidity limit, we obtain

$$\begin{aligned} B_{\pm}(a,b,c,d)&=A_{\pm}[\delta_{ac}-\delta_{bd}e^{[(a+c)/2-b\pm1]\eta}]\\ &=0,\quad (a-b)(b-c)(c-d)(a-d)\neq\pm1\ , \end{aligned} \tag{6.12}$$

where we have included a normalization factor $A_{\pm}$.

2. The cyclic SOS model

The q-state cyclic SOS model (Pearce and Seaton, 1988, 1989) is characterized by the Dynkin diagram $A_q^{(1)}$ of Fig. 41. The contributing configurations are also those shown in Fig. 45, but now with indices $a,b,\ldots,$ mod(q). The critical vertex weights are again those given by Eqs. (6.10) and (6.11), but with

$$\eta=i2\pi s/q,\quad s=1,2,\ldots,q-1\ . \tag{6.13}$$

Since the q states are cyclic, the partition function is independent of the height of the exterior face, and we have $Z_{\rm IRF}(B)=qZ_{\rm IRF}(a)(B)$.

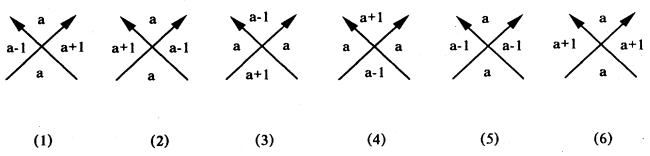

FIG. 45. Configurations of the ABF and cyclic solid-on-solid (SOS) models.

E. Enhanced IRF models

Analogous to the discussions in Sec. IV.C, we introduce the piecewise-linear lattice $\mathcal{L}^*$ and *enhanced* IRF models on $\mathcal{L}^*$. The enhanced IRF model has angle-dependent Boltzmann weights

$$B^*(a,b,c,d|u)=\lambda^{(h_{da}-h_{cb})\theta/2\pi}B(a,b,c,d|u)\ , \tag{6.14}$$

where θ is the angle of the two edges bordering the face indexed a, and, for vertices of degree 2 on $\mathcal{L}^*$,

$$\begin{aligned} B^*(a,b)&=\lambda^{h_{ab}\theta/2\pi}\quad\text{if the line turns an angle }\theta\\ &\qquad\text{to the left}\\ &=\lambda^{-h_{ab}\theta/2\pi}\quad\text{if the line turns an angle }\theta\\ &\qquad\text{to the right}\\ &=0\quad\text{if adjacent heights } a \text{ and } b \text{ are forbidden.} \end{aligned} \tag{6.15}$$

Here the arrangement of a and b is the same as in Fig. 42. This enhanced IRF model now maps into an enhanced vertex model with vertex weights as in Eqs. (4.17a) and (4.17b) and the replacement of a by $f(a)$.

The partition function of the enhanced IRF model is now

$$Z_{\rm IRF}(B^*)=\sum_{\{\text{heights}\}}\prod B^*(a,b,c,d,|u)\prod B^*(a,b)\ , \tag{6.16}$$

and, in the infinite-rapidity limit,

$$Z_{\rm IRF}(B^*_{\pm})=\sum_{\{\text{heights}\}}\prod B^*_{\pm}(a,b,c,d)\prod B^*(a,b)\ , \tag{6.17}$$

where

$$B^*_{\pm}(a,b,c,d)=\lambda^{(h_{da}-h_{cb})\theta/2\pi}B_{\pm}(a,b,c,d)\ . \tag{6.18}$$

The creation of vertices of degree two leads to the consideration of lattices in the form of a ring. We shall assume that the integer set $\mathcal{I}$ and the function f have been chosen such that the partition function of a ring,

$$Z_{\rm ring}(B^*)=\sum_{\{a,b\}\in\mathcal{I}}\lambda^{\pm h_{ab}}=\Lambda\ , \tag{6.19}$$

is a constant. Here the summation is taken over heights a and b, consistent with the adjacency requirement.

F. Construction of knot invariants

We now construct knot invariants from IRF models. From a given knot we consider an integrable IRF model

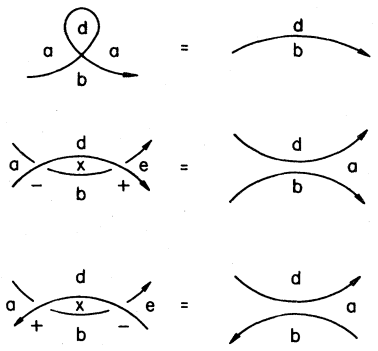

FIG. 46. Reidemeister moves I and II for IRF models.

and its equivalent enhanced vertex model. We can then use Theorem V.A.1, and, since the equivalent vertex model is charge conserving, we need only consider conditions (5.1a)–(5.3a). Recasting these conditions for Reidemeister moves I and II in terms of Boltzmann weights $B_{\pm}(a,b,c,d)$, a process we show in Fig. 46, we obtain

$$\sum_{d\in\mathcal{J}} \lambda^{f(d)-f(a)} B_{\pm}(a,b,a,d)=1, \quad \text{for all } a,b. \quad \text{(I)}, \tag{6.20a}$$

$$\sum_{x\in\mathcal{J}} B_{\pm}(a,b,x,d)B_{\mp}(x,b,e,d)=\delta_{ae} \quad \text{(IIA)}, \tag{6.20b}$$

$$\sum_{x\in\mathcal{J}} \lambda^{f(a)+f(x)-f(b)-f(d)} B_{\pm}(d,a,b,x) \times B_{\mp}(b,e,d,x)=\delta_{ae} \quad \text{(IIB)}. \tag{6.20c}$$

These conditions have been obtained by Akutsu *et al.* (1988). Note that, as in the case of vertex models, Eq. (6.20b) is a consequence of the unitarity condition, Eq. (6.7).

We now state our results on IRF models as a theorem:

Theorem VI.F. For each oriented knot we construct a directed lattice $\mathcal{L}$ and the associated piecewise-linear lattice $\mathcal{L}^*$. Then the partition function (6.17) of an enhanced IRF model with Boltzmann weights (6.15) and (6.18) is a knot invariant, provided that Eqs. (6.20a)–(6.20c) hold and that the partition function of an unknot is Eq. (6.19).

G. Examples

We now apply Theorem VI.F to the ABF and cyclic SOS models, both of which lead to the Jones polynomial (Akutsu and Wadati, 1988).

Using the Boltzmann weight given by Eq. (6.12), we find that Eq. (6.20a) is satisfied by choosing

$$f(a)=a, \quad \lambda=e^{\eta}, \quad A_{\pm}=e^{\mp\eta}. \tag{6.21}$$

With these choices, one readily verifies that both Eqs. (6.20b) and (6.20c) hold and that the partition function of a ring, Eq. (6.19), is $\Lambda=e^{\eta}+\epsilon^{-\eta}$ for the ABF model and $\Lambda=q(e^{\eta}+\epsilon^{-\eta})$ for the cyclic SOS model. It follows that $Z(B_{\pm}^*)$ is a knot invariant.

To identify this invariant as the Jones polynomial, we obtain from Eqs. (6.12), (6.14), and (6.21) the identity

$$e^{-2\eta}B_{+}^*(a,b,c,d)-e^{2\eta}B_{-}^*(a,b,c,d) =(-e^{\eta}+\epsilon^{-\eta})e^{(d-a)\theta/2\pi}e^{-(a-b)\theta/2\pi} \times\delta_{d-a,d-c}\delta_{a-b,c-b}. \tag{6.22}$$

This is precisely Eq. (5.22) leading to the Skein relation (2.6) for the Jones polynomial $V(t)$ after identifying $e^{\eta}=-\sqrt{t}$. This establishes that

$$V(t)=\Lambda^{-1}Z(B_{\pm}^*). \tag{6.23}$$

By considering multicomponent spins, Akutsu *et al.* (1989) have shown that the Homfly and Kauffman polynomials can also be constructed from IRF models.

VII. KNOT INVARIANTS FROM EDGE-INTERACTION MODELS

A. Formulation

In our discussion of constructing knot invariants from IRF models, we have not inquired about explicit realizations of the Boltzmann weight $B(a,b,c,d)$. In this section we consider the realization of B by explicitly introducing two-spin interactions. While it is possible to do this by further specializing our results on IRF models, it is more convenient to take advantage of the simplicity of the interaction and proceed directly. This direct approach also eliminates the need for introducing the piecewise-linear lattice $\mathcal{L}^*$ and the associated enhanced lattice models. This leads to the consideration of edge-interaction models.

Starting from a given knot consisting of N line crossings, we construct an *unoriented* lattice $\mathcal{L}$ of N sites, while disregarding the line orientations. In the simplest case we consider a spin model whose spins reside in one set of the bipartite faces of $\mathcal{L}$ forming a lattice $\mathcal{L}'$.[19] To help us visualize, it is convenient to shade faces of $\mathcal{L}$ containing spins, a device first introduced by Baxter *et al.* (1976) in an analysis of the Potts model for arbitrary planar lattices.[20] An example of a lattice $\mathcal{L}$ with shaded

[19]It is also possible to consider spin models (Jones, 1989) whose spins reside in all faces of $\mathcal{L}$. If the four spins surrounding a vertex of $\mathcal{L}$ interact with crossing pair interactions, then the two sets of spins are decoupled and the overall partition function becomes a product of two, one for each sublattice (Kadanoff and Wegner, 1971; Wu, 1971).

[20]The designations of $\mathcal{L}$ and $\mathcal{L}'$ here are interchanged from that in Baxter *et al.* (1976).

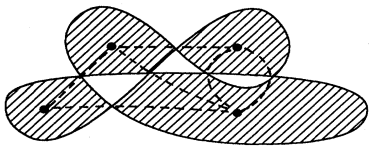

FIG. 47. Example of a lattice for a spin model with pure pair interactions. The solid circles denote spins and the dashed lines denote lattice edges and interactions.

faces is shown in Fig. 47. The lattice $\mathcal{L}$ is the surrounding, or the covering, lattice of $\mathcal{L}'$.

Let the spins interact with two-spin interactions placed across lattice sites of $\mathcal{L}$ (and along lattice edges of $\mathcal{L}'$) as indicated by the dashed lines in Fig. 47. Then, depending on the relative positionings of the shaded faces with respect to the line crossing, we assign two kinds of interactions, + and −, as shown in Fig. 48.[21]

We let the Boltzmann factors be $W_{\pm}(a,b)$, and, for simplicity, we assume symmetric interactions, i.e.,

$$W_{\pm}(a,b)=W_{\pm}(b,a)\ . \tag{7.1}$$

As in the case of the IRF model, we assume that spin variables $a,b,\ldots$ take on q integral values in the set $\mathcal{J}$. The partition function (3.1) now reads

$$Z(W_{\pm})=q^{-N/2}\sum_{\text{spin states}}\prod W_{\pm}(a,b)\ , \tag{7.2}$$

where the product is over all interacting spin pairs in $\mathcal{L}'$, and we have introduced to each spin summation[22] a factor $q^{-1/2}$. The partition function of a single spin corresponding to an unknot is then

$$Z_{\text{single spin}}=q^{-1/2}\sum_{a\in\mathcal{J}}1=\sqrt{q}\ . \tag{7.3}$$

We require the partition function $Z(W_{\pm})$ to be an invariant of regular isotopy under Reidemeister moves of lattice edges. Taking into account all possible face shadings, this leads to the independent moves shown in Figs. 49 and 50. Figure 49 shows the four independent Reidemeister moves I of regular isotopy derived by shading faces of the two type-I moves shown in Fig. 13 and Eq. (2.15). Similarly, Fig. 50 contains independent Reidemeister moves of types II and III derived by shading faces of the corresponding moves in Fig. 3. Explicitly, the conditions are

$$\frac{1}{\sqrt{q}}\sum_{b\in\mathcal{J}}W_{\pm}(a,b)=\alpha^{\mp 1}\ , \tag{7.4}$$

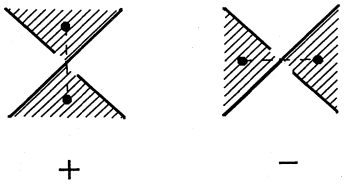

FIG. 48. Two kinds of interactions in the spin model. The interaction is of type + (−) if one finds the shaded area on the left (right) upon leaving the vertex along an edge that is an "overpass."

$$W_{\pm}(a,a)=\alpha^{\pm 1}\ , \tag{7.5}$$

for Reidemeister moves I, and

$$\frac{1}{\sqrt{q}}\sum_{b\in\mathcal{J}}W_{-}(a,b)W_{+}(b,c)=\sqrt{q}\,\delta_{ac}\ , \tag{7.6}$$

$$W_{+}(a,b)W_{-}(a,b)=1\ , \tag{7.7}$$

$$\frac{1}{\sqrt{q}}\sum_{d\in\mathcal{J}}W_{\pm}(a,d)W_{\mp}(b,d)W_{\pm}(c,d)=W_{\mp}(a,b)W_{\mp}(b,c)W_{\pm}(c,a) \tag{7.8}$$

for Reidemeister moves II and III.[23] Conditions (7.4)–(7.8) can be more conveniently represented by linear graphs on $\mathcal{L}'$, as shown in Fig. 51.

Note that according to Eq. (7.2) there is a factor $q^{-1/2}$ for each shaded area; this leads to the compensating factors occurring in the left-hand side of Eqs. (7.4), (7.6), and (7.8). Furthermore, conditions (7.4)–(7.8) are not all independent. Setting $b=c$ in Eq. (7.8), for example, one obtains Eq. (7.4) after using Eqs. (7.5) and (7.7). The condition (7.8) is the Yang-Baxter equation, which is a generalization of the star-triangle equation for the Ising model (Onsager, 1944).

We now state the main result as a theorem:

Theorem VII.A. For each knot we construct an unoriented lattice $\mathcal{L}$ and a q-state spin model with spins occupying every other face of $\mathcal{L}$, with its partition function $Z(W_{\pm})$ given by Eqs. (7.2). Then $q^{-1/2}Z(W_{\pm})$ is an invariant of regular isotopy for unoriented knots satisfying Eqs. (2.14) and (2.15), provided that Eqs. (7.4)–(7.8) hold.

Corollary VII.A. The function $\alpha^{-w(K)}Z(W_{\pm})/\sqrt{q}$ is an invariant of ambient isotopy for oriented knots.

Finally, we remark that since the faces of $\mathcal{L}$, or the lattice $\mathcal{L}'$, are bipartite, there exist two choices for shading the faces, and hence two ways of constructing the spin model. However, these two choices lead to the same invariant (Jones, 1989).

[21]It should be noted that the + and − types of vertices in this context are different from the + and − types of crossings introduced in Sec. II.

[22]More generally one introduces a factor $\tau^{-1/2}$ for each summation. Then setting $a=c$ in Eq. (7.6) and using Eq. (7.7), one obtains $\tau=q$.

[23]The condition imposed by Reidemeister moves III must now be checked, since we are not basing our derivation on solutions of the Yang-Baxter equation.

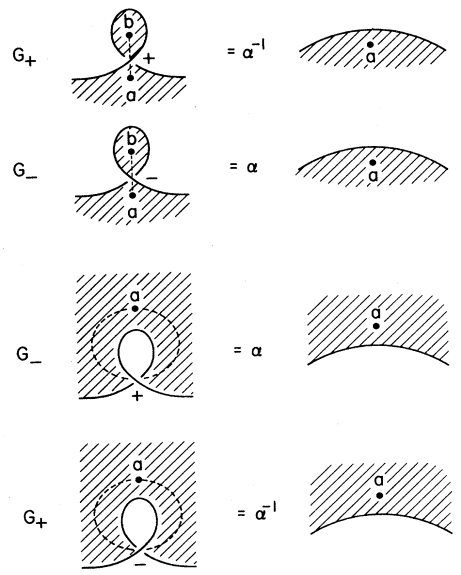

FIG. 49. Type-I Reidemeister moves.

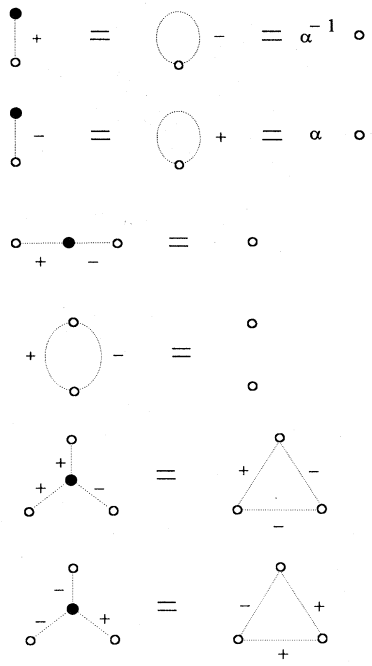

FIG. 51. Equivalent representations of Reidemeister moves. Open circles are rooted denoting fixed spin states; solid circles denote spin states under summations.

B. Example

As an example of the formulation, we show that the Potts model leads to the Jones polynomial (Kauffman, 1988b).

The Potts model (Potts, 1952; for a review see Wu, 1982) is characterized by the two-spin Boltzmann factor

$$W_{\pm}(a,b)=A_{\pm}e^{K_{\pm}\delta_{ab}} =A_{\pm}(1+v_{\pm}\delta_{ab})\ , \tag{7.9}$$

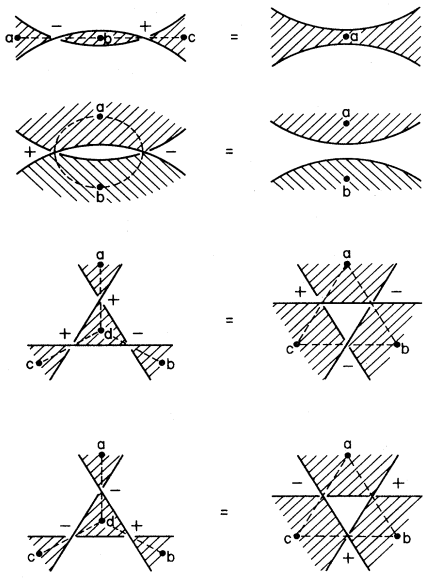

FIG. 50. Type-II and type-III Reidemeister moves.

where

$$v_{\pm}=e^{K_{\pm}}-1\ . \tag{7.10}$$

Then the substitution of Eq. (7.9) into Eq. (7.7) leads to

$$A_{+}A_{-}=1,\quad v_{+}+v_{-}+v_{+}v_{-}=0\ . \tag{7.11}$$

The second relation in Eq. (7.11) corresponds to $K_{+}=-K_{-}$. Similarly, Eq. (7.6) leads, after using Eq. (7.11), to

$$q=v_{+}v_{-}\ , \tag{7.12}$$

and Eq. (7.8) leads to

$$A_{\pm}^{2}=\sqrt{q}\ /v_{\pm}\ . \tag{7.13}$$

Finally, it can be checked that both Eqs. (7.4) and (7.5) are satisfied if one takes

$$\alpha=A_{+}(1+v_{+})=[A_{-}(1+v_{-})]^{-1}\ . \tag{7.14}$$

It is readily verified that Eqs. (7.11)–(7.14) are satisfied by writing

$$\begin{aligned} &t\equiv -e^{-K_{+}}=-e^{K_{-}}\ ,\\ &v_{\pm}=-(1+t^{\mp 1})\ ,\\ &A_{\pm}=t^{\pm 1/4}\ ,\\ &q=t+2+1/t\ ,\\ &\alpha=-t^{-3/4}\ . \end{aligned} \tag{7.15}$$

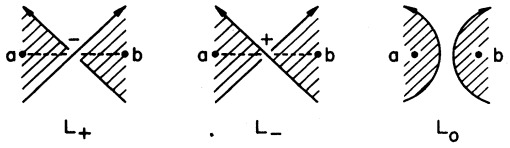

FIG. 52. Skein relation configurations. Note that the W_+ (W_-) interaction corresponds to the L_- (L_+) crossing.

Then, by Theorem VII.A, $Z(W_\pm)$ is an invariant for unoriented knots, and, by Corollary VII.A, $P(t)=(-t^{-3/4})^{-w(K)}Z(W_\pm)$ is an invariant for oriented knots. To identify $P(t)$ as the Jones polynomial other than a normalization factor, we consider the three configurations shown in Fig. 52. A moment's reflection shows that $Z(W_\pm)$ satisfies the Skein relation (2.6), provided that we have [compare with Eq. (5.33)]

$$\frac{1}{t}[\alpha^{-1}W_-(a,b)]-t[\alpha W_+(a,b)]=\sqrt{t}-\frac{1}{\sqrt{t}}\ . \qquad (7.16)$$

Indeed, using Eq. (7.15) one verifies that Eq. (7.16) is an identity. Now $P(t)$ has $P_{\text{unknot}}(t)=\sqrt{q}$ as a factor. We thus conclude that

$$V(t)=q^{-1/2}(-t^{-3/4})^{w(K)}Z(W_\pm) \qquad (7.17)$$

is a Laurent polynomial normalized to $V_{\text{unknot}}(t)=1$ and is thus the Jones polynomial.

For further examples of invariants derived from spin models with pure two-spin interactions, see Jones (1989).

VIII. SUMMARY

We have presented the formulation of knot invariants using the method of two-dimensional models in statistical mechanics. The underlying theme of the statistical mechanical approach is the construction of lattice models on lattices deduced from planar projections of knots, with the requirement that the partition function remain invariant under Reidemeister moves of lattice edges. When this is done, the partition function is a knot invariant.

The requirement of invariance under Reidemeister moves leads naturally to the consideration of integrable lattice models. It is shown that the integrability of a lattice model leads to invariance under two of the required Reidemeister moves, namely, IIIA and IIA. Then the job is done if the remaining Reidemeister moves, I and IIB, are also realized.

The main results using vertex and IRF models are summarized in Theorems V.A.1 and VI.F, respectively. The construction of knot invariants can also be carried out using spin models with pure two-spin interactions. This leads to Theorem VII.A and the semioriented invariants.

Finally, we emphasize that the approach presented in this review utilizes lattice models whose Boltzmann weights are strictly *local,* without reference to global considerations. Such considerations of local Boltzmann factors are in line with conventional statistical mechanics. With this perspective in mind, we have presented a genuine statistical mechanical approach to knot invariants.

ACKNOWLEDGMENTS

I am grateful to C. King for a critical reading of the manuscript and for comments and suggestions that have greatly improved the clarity of the presentation. I am also indebted to J. H. H. Perk for critical and helpful comments and for calling my attention to relevant references. I would like to thank L. H. Kauffman for sending me a copy of his book (Kauffman, 1991) prior to publication, and V. F. R. Jones for comments. The knot table of Fig. 53 is produced from computer graphics designed by D. Rolfsen and R. Scharein; I am grateful to D. Rolfsen for providing a copy of the figure for our use. This work is supported in part by the National Science Foundation Grant DMR-9015489.

APPENDIX: TABLE OF KNOT INVARIANTS

Traditionally, knots are classified according to the minimum number of crossings in a planar projection. Prime knots and links with up to thirteen crossings have been tabulated in Thistlethwaite (1985). Here we include in Fig. 53 graphs of prime knots and links with up to six

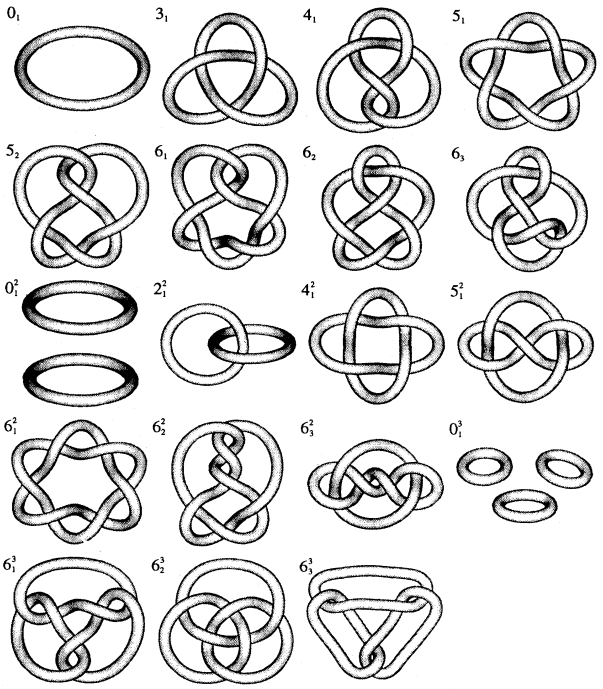

FIG. 53. Planar projections of prime knots and links with six or fewer crossings.

crossings. We also include a table of the associated polynomial invariants. The knot notation of 6_2^3, for example, denotes the second three-component knot (link) with six crossings. In the case of links for which there exist more than one orientation, only those generating distinct invariants are given. They are specified by the subscript $i=1,2$ in $[\ ]_i$. Our convention of specifying the subscript is that if $w_i(K)$ is the writhe of the oriented knot $[K]_i$, $i=1,2$, then $w_2(K)>w_1(K)$.

1. The Alexander-Conway polynomial

The Alexander-Conway polynomial $\Delta(t)=\nabla(z)$, $z=\sqrt{t}-1/\sqrt{t}$, is defined in Sec. II.D.1. Further listings of the Alexander polynomial can be found in Burde and Zieschang (1985) and Rolfsen (1976).

0_1	1	
3_1	$t^{-1}(1-t+t^2)$	$=1+z^2$
4_1	$t^{-1}(-1+3t-t^2)$	$=1-z^2$
5_1	$t^{-2}(1-t+t^2-t^3+t^4)$	$=1+3z^2+z^4$
5_2	$t^{-1}(2-3t+2t^2)$	$=1+2z^2$
6_1	$t^{-1}(-2+5t-2t^2)$	$=1-2z^2$
6_2	$t^{-2}(-1+3t-3t^2+3t^3-t^4)$	$=1-z^2-z^4$
6_3	$t^{-2}(1-3t+5t^2-3t^3-t^4)$	$=1+z^2+z^4$

Alexander polynomials for links with two or more components vanish identically.

2. The Jones polynomial

The Jones polynomial $V(t)$ listed below is defined in Sec. II.D.2 and is the same as in Jones (1987). Further listings of the Jones polynomial for single-component knots can be found in Jones (1985, 1987). Note, however, definitions of $V(t)$ in Jones (1985) and Jones (1987) are related by $t\to t^{-1}$, and expressions in Jones (1985) contain several misprints.[24]

0_1	1
3_1	$t^{-4}(-1+t+t^3)$
4_1	$t^{-2}(1-t+t^2-t^3+t^4)$
5_1	$t^{-7}(-1+t-t^2+t^3+t^5)$
5_2	$t^{-6}(-1+t-t^2+2t^3-t^4+t^5)$
6_1	$t^{-4}(1-t+t^2-2t^3+2t^4-t^5+t^6)$
6_2	$t^{-5}(1-2t+2t^2-2t^3+2t^4-t^5+t^6)$
6_3	$t^{-3}(-1+2t-2t^2+3t^3-2t^4+2t^5-t^6)$
0_1^2	$t^{-1/2}(-1-t)$
2_1^2	$t^{-5/2}(-1-t^2)$
$[4_1^2]_1$	$t^{-11/2}(-1+t-t^2-t^4)$
$[4_1^2]_2$	$\sqrt{t}\,(-1+t-t^2-t^4)$
5_1^2	$t^{-7/2}(1-2t+t^2+2t^3+t^4-t^5)$
$[6_1^2]_1$	$t^{-17/2}(-1+t-t^2+t^3-t^4-t^6)$
$[6_1^2]_2$	$\sqrt{t}\,(-1+t-t^2+t^3-t^4-t^6)$
6_2^2	$t^{3/2}(-1+t-2t^2-2t^3+2t^4+t^5-t^6)$
$[6_3^2]_1$	$t^{-15/2}(-1+2t-2t^2+2t^3-3t^4+t^5-t^6)$
$[6_3^2]_2$	$t^{-3/2}(-1+2t-2t^2+2t^3-3t^4+t^5-t^6)$
0_1^3	$t^{-1}(1+2t+t^2)$
$[6_1^3]_1$	$t^{-1}(1-t+3t^2-t^3+3t^4-2t^5+t^6)$
$[6_1^3]_2$	$t^{-7}(1-t+3t^2-t^3+3t^4-2t^5+t^6)$
6_2^3	$t^{-3}(-1+3t-2t^2+4t^3-2t^4+3t^5-t^6)$
$[6_3^3]_1$	$t^{-4}(1+t^2+2t^4)$
$[6_3^3]_2$	$t^2(1+t^2+2t^4)$

3. The Homfly polynomial

The Homfly polynomial $P(t,z)$ given below is defined in Sec. II.D.3 and computed from the list of $P(l,m)$ given by Lickorish and Millett (1987, 1988), by substituting with $l=it^{-1}$, $m=iz$. Setting $z=\sqrt{t}-1/\sqrt{t}$ in the expressions below we recover the Jones polynomial, and setting $t=1$ we recover the Alexander-Conway polynomial.

0_1	1
3_1	$t^{-4}(-1+2t^2+z^2t^2)$
4_1	$t^{-2}(1-t^2+t^4-t^2z^2)$
5_1	$t^{-6}[-2+3t^2+z^2(-1+4t^2)+t^2z^4]$
5_2	$t^{-6}[-1+t^2+t^4+z^2t^2(1+t^2)]$
6_1	$t^{-4}[1-t^2+t^6-t^2(1+t^2)z^2]$
6_2	$t^{-4}[1-2t^2+2t^4+(1-3t^2+t^4)z^2-t^2z^4]$
6_3	$t^{-2}(-1+3t^2-t^4)(1+z^2)+z^4$
0_1^2	$(zt)^{-1}(1-t^2)$
2_1^2	$(zt^3)^{-1}(1-t^2)-zt^{-1}$
$[4_1^2]_1$	$(zt^5)^{-1}(1-t^2)-3zt^{-3}(1-t^2)-z^3t^{-3}$
$[4_1^2]_2$	$(zt)^{-1}(1-t^2)-zt^{-3}(1-t^2)^2+z^3t^{-1}$
5_1^2	$(zt)^{-1}(1-t^2)-zt^{-3}(1-t^2)^2+z^3t^{-1}$
6_1^2	$(zt^7)^{-1}(1-t^2)+3zt^{-7}(1-2t^2)+z^3t^{-7}(1-5t^2)$ $-z^5t^{-5}$
6_2^2	$t^5z^{-1}(1-t^2)+zt^3(2+2t^2-t^4)+z^3t^3(1+t^2)$
$[6_3^2]_1$	$(t^5z)^{-1}(1-t^2)+zt^{-7}(1-t^2-2t^4)-z^3t^{-5}(1+t^2)$
$[6_3^2]_2$	$t^3z^{-1}(1-t^2)+zt^{-1}(1-t^2+2t^4)-tz^3$
0_1^3	$(zt)^{-1}(1-2t^2+t^4)$
$[6_1^3]_1$	$(1-t^2)z^{-2}+(1-3t^2+2t^4)+(1-3t^2+t^4)z^2$ $-t^2z^4$
$[6_1^3]_2$	$t^{-8}(1-t^2)^2z^{-2}+3t^{-6}(-1+t^2)+t^{-4}(2+t^2)z^2$
6_2^3	$t^{-2}(1-t^2)^2z^{-2}-t^{-2}(1-t^2)^2z^2+z^4$
$[6_3^3]_1$	$t^{-4}(1-t^2)^2z^{-2}+t^{-4}(1-3t^2+2t^4)-t^{-2}z^2$
$[6_3^3]_2$	$t^4(1-t^2)^2z^{-2}+3t^4(1-t^2)+t^4(4-t^2)z^4+t^4z^4$

[24]Specifically, the expression for 6_1 in Jones (1985) is in error (but correct in Jones, 1987), and expressions for the links 4_1^2 (the second expression), 5_1^2, 6_2^2, 6_3^2, 6_1^3, and 6_3^3 are given in the variable t^{-1}, instead of t. The expressions for 6_1^2 and 6_2^3 given in Jones (1985) are correct.

4. The three-state Akutsu-Wadati polynomial

The N-state Akutsu-Wadati polynomial $A^{(N)}(t)$ is defined in Sec. V.A.5. The following list of $A^{(3)}(t)$ for knots of closed three-braids is taken from Akutsu *et al.* (1987).

3_1 $t^2(1+t^3-t^5+t^6-t^7-t^8+t^9)$

4_1 $t^{-6}(1-t-t^2+2t^3-t^4-t^5+3t^6-t^7-t^8+2t^9-t^{10}-t^{11}+t^{12})$

5_1 $t^4(1+t^3-t^5+t^6-t^8+t^9-2t^{11}+t^{12}-t^{14}+t^{15})$

5_2 $t^2(1-t+3t^3-2t^4-t^5+4t^6-3t^7-t^8+3t^9-2t^{10}-t^{11}+2t^{12}-t^{13}-t^{14}+t^{15})$

6_2 $t^{-4}(1-t-t^2+3t^3-t^4-3t^5+5t^6-t^7-5t^8+6t^9-6t^{11}+6t^{12}-5t^{14}+4t^{15}-2t^{17}+t^{18})$

6_3 $t^{-9}(1-2t-t^2+5t^3-4t^4-3t^5+9t^6-5t^7-5t^8+11t^9-5t^{10}-5t^{11}$
$+9t^{12}-3t^{13}-4t^{14}+5t^{15}-t^{16}-2t^{17}+t^{18})$

5. The Kauffman polynomial—the Dubrovnik version

The Kauffman polynomial $L(\alpha,z)$ is defined in Sec. II.D.5. In the following we list $Q(\alpha,z)$, the Dubrovnik version of the Kauffman polynomial, computed from the list of $L(\alpha,z)$ given by Kauffman (1987b) and using Eq. (2.16).

3_1 1

3_1 $(2\alpha-\alpha^{-1})+(1-\alpha^{-2})z+(\alpha-\alpha^{-1})z^2$

4_1 $(\alpha^2-1+\alpha^{-2})+(-\alpha+\alpha^{-1})z+(\alpha^2-2+\alpha^{-2})z^2+(-\alpha+\alpha^{-1})z^3$

5_1 $(3\alpha-2\alpha^{-1})+(2-\alpha^{-2}-\alpha^{-4})z+(4\alpha-3\alpha^{-1}-\alpha^{-3})z^2+(1-\alpha^{-2})z^3+(\alpha-\alpha^{-1})z^4$

5_2 $(-\alpha+\alpha^{-1}+\alpha^{-3})+(-2+2\alpha^{-2})z+(-2\alpha+\alpha^{-1}+\alpha^{-3})z^2+(\alpha^2-2+\alpha^{-2})z^3+(-\alpha+\alpha^{-1})z^4$

6_1 $(-\alpha^2+1-\alpha^{-4})+2(\alpha-\alpha^{-1})z+(-3\alpha^2+4-\alpha^{-4})z^2$
$+(-3\alpha+2\alpha^{-1}+\alpha^{-3})z^3+(\alpha^2-2+\alpha^{-2})z^4+(-\alpha+\alpha^{-1})z^5$

6_2 $(-2\alpha^2+2+\alpha^{-2})+(\alpha^{-1}-\alpha^{-3})z+(-3\alpha^2+6-2\alpha^{-2}-\alpha^{-4})z^2$
$+(-2\alpha+2\alpha^{-3})z^3+(\alpha^2-3+2\alpha^{-2})z^4+(-\alpha+\alpha^{-1})z^5$

6_3 $(-\alpha^2+3-\alpha^{-2})+(\alpha^3-2\alpha+2\alpha^{-1}-\alpha^{-3})z+(-3\alpha^2+6-3\alpha^{-2})z^2$
$+(\alpha^3-\alpha+\alpha^{-1}-\alpha^{-3})z^3+(-2\alpha^2+4-2\alpha^{-2})z^4+(\alpha-\alpha^{-1})z^5$

0_1^2 $1+(\alpha-\alpha^{-1})z^{-1}$

0_1^3 $[1+(\alpha-\alpha^{-1})z^{-1}]^2$

REFERENCES

Akutsu, Y., T. Deguchi, and M. Wadati, 1987, "Exactly solved models and new link polynomials. II. Link polynomials for closed 3-braids," J. Phys. Soc. Jpn. **56**, 3464–3479.

Akutsu, Y., T. Deguchi, and M. Wadati, 1988, "Exactly solved models and new link polynomials. IV. IRF models," J. Phys. Soc. Jpn. **57**, 1173–1185.

Akutsu, Y., T. Deguchi, and M. Wadati, 1989, "The Yang-Baxter relation: a new tool for knot theory," in *Braid Group, Knot Theory, and Statistical Mechanics,* edited by C. N. Yang and M. L. Ge (World Scientific, Singapore), pp. 151–200.

Akutsu, Y., A. Kuniba, and M. Wadati, 1986a, "Exactly solvable IRF models. II. S_N-generalizations," J. Phys. Soc. Jpn. **55**, 1466–1474.

Akutsu, Y., A. Kuniba, and M. Wadati, 1986b, "Exactly solvable IRF models. III. A new hierarchy of solvable models," J. Phys. Soc. Jpn. **55**, 1466–1474.

Akutsu, Y., and M. Wadati, 1987a, "Knot invariants and the critical statistical systems," J. Phys. Soc. Jpn. **56**, 839–842.

Akutsu, Y., and M. Wadati, 1987b, "Exactly solvable models and new link polynomials. I. N-state vertex models," J. Phys. Soc. Jpn. **56**, 3039–3051.

Alexander, J. W., 1928, "Topological invariants of knots and knots," Trans. Am. Math. Soc. **30**, 275–306.

Andrews, G. E., R. J. Baxter, and P. J. Forrester, 1984, "Eight-vertex SOS model and generalized Rogers-Ramanujan-type identities," J. Stat. Mech. **35**, 193–266.

Baxter, R. J., 1971, "Eight-vertex model in lattice statistics," Phys. Rev. Lett. **26**, 832-833.

Baxter, R. J., 1972, "Partition function of the eight-vertex lattice model," Ann. Phys. (N.Y.) **70**, 193–228.

Baxter, R. J., 1973a, "Eight-vertex model in lattice statistics and one-dimensional anisotropic Heisenberg chain. I. Some fundamental eigenvectors," Ann. Phys. (N.Y.) **76**, 1–24.

Baxter, R. J., 1973b "Eight-vertex model in lattice statistics and one-dimensional anisotropic Heisenberg chain. II. Equivalence to a general ice-type lattice model," Ann. Phys. (N.Y.) **76**, 25–47.

Baxter, R. J., 1978, "Solvable eight-vertex model on an arbitrary planar lattice," Philos. Trans. R. Soc. London **289**, 315–346.

Baxter, R. J., 1980, "Exactly solved models," in *Fundamental Problems in Statistical Mechanics V,* edited by E. G. D. Cohen (North-Holland-Amsterdam), pp. 109–141.

Baxter, R. J., 1982, *Exactly Solved Models in Statistical Mechanics* (Academic, New York).

Baxter, R. J., S. B. Kelland, and F. Y. Wu, 1976, "Equivalence of the Potts model or Whitney polynomial with an ice-type model," J. Phys. A **9**, 397–406.

Bazhanov, V. V., 1985, "Trigonometric solutions of the star-

triangle equation and classical Lie algebras," Phys. Lett. B **159**, 321–324.
Birman, J. S., 1985, "On the Jones polynomial of closed 3-braids," Invent. Math. **81**, 287–294.
Burde, G., and H. Zieschang, 1985, *Knots* (Walter de Gruyter, New York).
Conway, J. H., 1970, "An enumeration of knots and links and some of their algebraic properties," in *Computational Problems in Abstract Algebra,* edited by J. Leech (Pergamon, New York), pp. 329–358.
Date, E., M. Jimbo, T. Miwa, and M. Okado, 1986, "Fusion of the eight-vertex SOS model," Lett. Math. Phys. **12**, 209–215.
Deguchi, T., Y. Akutsu, and M. Wadati, 1988, "Exactly solvable models and new link polynomials. III. Two-variable topological invariants," Phys. Soc. Jpn. **57**, 757–776.
Drinfel'd, V. G., 1986, "Quantum groups," in *Proceedings of the International Congress of Mathematicians,* Berkeley, edited by A. M. Gleason (Academic, New York), pp. 798–820.
Fan, C., and F. Y. Wu, 1970, "General lattice statistical model of phase transitions," Phys. Rev. B **2**, 723–733.
Fortuin, C. M., and P. W. Kasteleyn, 1972, "On the random-cluster model I. Introduction and relation to other models," Physica **57**, 536–564.
Freyd, P., D. Yetter, J. Hoste, W. B. R. Lickorish, K. C. Millett, and A. Oceanau, 1985, "A new polynomial invariant of knots and links," Bull. Am. Math. Soc. **12**, 239–246.
Gaudin, M., 1967, "Un système à une dimension de fermions en interaction," Phys. Lett. A **24**, 55-56.
Ge, M. L., L. Y. Wang, K. Xue, and Y. S. Wu, 1989, "Akutsu-Wadati polynomials from Feynman-Kauffman diagrams," in *Braid Group, Knot Theory, and Statistical Mechanics,* edited by C. N. Yang and M. L. Ge (World Scientific, Singapore), pp. 201–237.
Hoste, J., 1986, "A polynomial invariant for knots and links," Pacific J. Math. **124**, 295–320.
Ising, E., 1925, "Beitrag zur theorie des ferromagnetismus," Z. Phys. **31**, 253–258.
Jimbo, M., 1986, "Quantum R matrix for the generalized Toda system," Commun. Math. Phys. **102**, 537–547.
Jimbo, M., 1989, *Yang-Baxter Equation in Integrable Systems* (World Scientific, Singapore).
Jimbo, M., T. Miwa, and M. Okado, 1988, "Solvable lattice models related to the vector representation of classical simple Lie algebras," Commun. Math. Phys. **116**, 507–525.
Jones, V. F. R., 1985, "A polynomial invariant for links via von Neumann algebras," Bull. Am. Math. Soc. **12**, 103–112.
Jones, V. F. R., 1987, "Hecke algebra representations of braid groups and link polynomials," Ann. Math. **126**, 103–112.
Jones, V. F. R., 1989, "On knot invariants related to some statistical mechanical models," Pacific J. Math. **137**, 311–334.
Jones, V. F. R., 1990a, "Knot theory and statistical mechanics," Sci. Am. November, 98–103.
Jones, V. F. R., 1990b, "Baxterization," Int. J. Mod. Phys. B **4**, 701–713.
Kadanoff, L. P., and F. J. Wegner, 1971, "Some critical properties of the eight-vertex model," Phys. Rev. B **4**, 3989–3993.
Kauffman, L. H., 1987a, "State models and the Jones polynomial," Topology **26**, 395–407.
Kauffman, L. H., 1987b, *On Knots* (Princeton University, Princeton, NJ).
Kauffman, L. H., 1988a, "New invariants in the theory of knots," Am. Math. Monthly **95**, 195–242.
Kauffman, L. H., 1988b, "Statistical mechanics and the Jones polynomial," Contemp. Math. **78**, 263–312.
Kauffman, L. H., 1990, "An invariant of regular isotopy," Trans. Am. Math. Soc. **318**, 417–471.
Kauffman, L. H., 1991, *Knots and Physics* (World Scientific, Singapore).
Kohno, T., 1991, *New Developments in the Theory of Knots* (World Scientific, Singapore).
Kulish, P. P., N. Y. Reshetkhin, and E. K. Sklyanin, 1981, "Yang-Baxter equation and representation theory. I," Lett. Math. Phys. **5**, 393–403.
Kulish, P. P., and E. K. Sklyanin, 1980, "On the solution of the Yang-Baxter equation," Zap. Nauchn. Semin. Lenningr. Otd. Mat. Inst. Steklova **95**, 129–160 (in Russian).
Kulish, P. P., and E. K. Sklyanin, 1982, "Solutions of the Yang-Baxter equation," J. Sov. Math. **19**, 1596-1620.
Kulish, P. P., and E. K. Sklyanin, 1982b, "Quantum spectral transform method. Recent developments," in *Integrable Quantum Field Theories,* edited by J. Hietarinta and C. Montonen, Lecture Notes in Physics Vol. 151 (Springer, Berlin), pp. 61–119.
Kuniba, A., Y. Akutsu, and M. Wadati, 1986a, "Exactly solvable IRF models. I. A three-state model," J. Phys. Soc. Jpn. **55**, 1092–1101.
Kuniba, A., Y. Akutsu, and M. Wadati, 1986b, "Exactly solvable IRF models. IV. Generalized Rogers-Ramanujan identities and a solvable hierarchy," J. Phys. Soc. Jpn. **55**, 2166–2176.
Kuniba, A., Y. Akutsu, and M. Wadati, 1986c, "Exactly solvable IRF models. V. A further new hierarchy," J. Phys. Soc. Jpn. **55**, 2605–2617.
Kuniba, A., Y. Akutsu, and M. Wadati 1986d, "The Gordon-generalization hierarchy of exactly solvable IRF models," J. Phys. Soc. Jpn. **55**, 3338–3353.
Kuniba, A., Y. Akutsu, and M. Wadati, 1986e, "Inhomogeneous eight-vertex SOS model and solvable IRF hierarchies," J. Phys. Soc. Jpn. **55**, 2907–2910.
Lickorish, W. B. R., 1988, "Polynomials for links," Bull. London Math. Soc. **20**, 558–588.
Lickorish, W. B. R., and K. C. Millett, 1987, "A polynomial invariant of oriented links," Topology **26**, 107–141.
Lickorish, W. B. R., and K. C. Millett, 1988, "The new polynomial invariants of knots and links," Math. Magazine **61**, 3–23.
Lieb, E. H., 1967a, "Exact solution of the problem of the entropy of square ice," Phys. Rev. Lett. **18**, 692–694.
Lieb, E. H., 1967b, "Exact solution of the F model of an antiferroelectric," Phys. Rev. Lett. **18**, 1046–1048.
Lieb, E. H., 1967c, "Exact solution of the two-dimensional Slater KDP model of a ferroelectric," Phys. Rev. Lett. **19**, 108–110.
Lieb, E. H., 1967d, "Residue entropy of square ice," Phys. Rev. **162**, 162–171.
Lieb, E. H., and W. Liniger, 1963, "Exact analysis of an interacting Bose gas. I. The general solution and the ground state," Phys. Rev. **130**, 1605–1616.
Lieb, E. H., and F. Y. Wu, 1972, "Two-dimensional ferroelectric models", in *Phase Transitions and Critical Phenomena, Vol. I,* edited by C. Domb and M. S. Green (Academic, New York), pp. 331–490.
Lipson, A. S., 1992, "Some more states models for link invariants," Pacific J. Math. **152**, 337–346.
McGuire, J. B., 1964, "Studies of exactly solvable one-dimensional N-body problems," J. Math. Phys. **5**, 622–636.
Onsager, L., 1944, "Crystal statistics I. A two-dimensional model with an order-disorder transition," Phys. Rev. **65**, 117–149.

Pasquier, V., 1987a, "Two-dimensional critical systems labelled by Dynkin diagrams," Nucl. Phys. B **285**, [FS19], 162–172.

Pasquier, V., 1987b, "Exact solubility of the D_n series," J. Phys. A **20**, L217–L220.

Pearce, P., and K. A. Seaton, 1988, "Solvable hierarchy of cyclic solid-on-solid lattice models," Phys. Rev. Lett. **60**, 1347–1350.

Pearce, P., and K. A. Seaton, 1989, "Exact solution of cyclic solid-on-solid lattice models," Ann. Phys. (N.Y.) **193**, 326–366.

Perk, J. H. H., and C. L. Schultz, 1981, "New families of commuting transfer matrices in q-state vertex models," Phys. Lett. A **84**, 407–410.

Perk, J. H. H., and C. L. Schultz, 1983, "Families of commuting transfer matrices in q-state vertex models," in *Nonlinear Integrable Systems—Classical and Quantum Theory,* edited by M. Jimbo and T. Miwa (World Scientific, Singapore), pp. 137–152.

Perk, J. H. H., and F. Y. Wu, 1986a, "Nonintersecting string model and graphical approach: Equivalence with a Potts model," J. Stat. Phys. **42**, 727–742.

Perk J. H. H., and F. Y. Wu, 1986b, "Graphical approach to the nonintersecting string model: Star-triangle equation, inversion relation, and exact solution," Physica A **138**, 100–124.

Potts, R. B., 1952, "Some generalized order-disorder transformations," Proc. Cambridge Philos. Soc. **48**, 106–109.

Przytycki, J. H., and P. Traczyk, 1987, "Invariants of links of Conway type," Kobe J. Math. **4**, 115–139.

Reidemeister, K., 1948, *Knotentheorie* (Chelsea, New York); English translation, edited by L. F. Boron, C. D. Christenson, and B. A. Smith, *Knot Theory* (BCS Associates, Moscow, Idaho, 1983).

Reshetikhin, N.Y., and V. Turaev, 1991, "Invariants of three-manifolds via link polynomials and quantum groups," Invent. Math. **103**, 547–597.

Rolfsen, D., 1976, *Knots and Links* (Publish or Perish, Berkeley).

Schultz, D. L., 1981, "Solvable q-state models in lattice statistics and quantum field theory," Phys. Rev. Lett. **46**, 629–632.

Sogo, K., Y. Akutsu, and A. Takayuki, 1983, "New factorized S-matrix and its application to exactly solvable q-state model. I," Prog. Theor. Phys. **70**, 730-738.

Stroganov, Y. G., 1979, "A new calculation method for partition functions in some lattice models," Phys. Lett. A **74**, 116–118.

Sutherland, B., 1967, "Exact solution of a two-dimensional model for hydrogen-bonded crystals," Phys. Rev. Lett. **19**, 103–104.

Takhtadzhan, L. A., and L. D. Faddeev, 1979, "The quantum inverse problem method and the XYZ Heisenberg model," Uspekhi Mat. Nauk **34**(5), 13–63 (in Russian) [Russian Math. Surveys **34**(5), 11–68 (1979)].

Temperley, H. N. V., and E. H. Lieb, 1971, "Relations between the percolation and colouring problem and other graph-theoretical problems associated with regular planar lattice: some exact results for the percolation problem," Proc. R. Soc. London A **322**, 251–280.

Thistlethwaite, M. B., 1985, "Knot tabulations and related topics," in *Aspects of Topology,* edited by I. M. James and E. H. Kronheimer, London Mathematical Society Lecture Notes 93 (Cambridge University Press, London), pp. 1–76.

Truong, T. T., 1986, "Structure properties of a $Z(N^2)$-spin model and its equivalent $Z(N)$-vertex model," J. Stat. Phys. **42**, 349–379.

Turaev, V. G., 1988, "The Yang-Baxter equation and invariants of links," Invent. Math. **92**, 527–553.

Wadati, M., T. Deguchi, and Y. Akutsu, 1989, "Exactly solvable models and knot theory," Phys. Rep. **180**, 247–332.

Witten, E., 1989a, "Quantum field theory and the Jones polynomial," Commun. Math. Phys. **121**, 351–399

Witten, E., 1989b, "Gauge theories and integrable lattice models," Nucl. Phys. B **322**, 629–697.

Witten, E., 1990, "Gauge theories, vertex models, and quantum groups," Nucl. Phys. B **330**, 285–346.

Wu, F. Y., 1967, "Exactly soluble model of the ferroelectric phase transition in two dimensions," Phys. Rev. Lett. **18**, 605–607.

Wu, F. Y., 1968, "Remarks on the modified potassium dihydrogen phosphate model of a ferroelectric," Phys. Rev. **168**, 539–543.

Wu, F. Y., 1971, "Ising model with four-spin interactions," Phys. Rev. B **4**, 2312-2314.

Wu, F. Y., 1982, "The Potts Model," Rev. Mod. Phys. **54**, 235–268.

Wu, F. Y., 1992a, "Knot theory and statistical mechanics," in *Computer-Aided Statistical Physics,* AIP Conf. Proc. No. 248 (American Institute of Physics, New York), pp. 3–11.

Wu, F. Y., 1992b, "Jones polynomial as a Potts model partition function," J. Knot Theory and Its Ramifications **1**, 47–57.

Yang, C. N., 1967, "Some exact results for the many-body problem in one dimension with repulsive delta-function interaction," Phys. Rev. Lett. **19**, 1312-1314.

Yang, C. N., and M. L. Ge, 1989, *Braid Group, Knot Theory, and Statistical Mechanics* (World Scientific, Singapore).

Zamolodchikov, A. B., 1979, "Z_4-symmetric factorized S-matrix in two space-time dimensions," Commun. Math. Phys. **69**, 165–178.

Zamolodchikov, A. B., and V. A. Fateev, 1980, "A model factorized S-matrix and an integrable spin-1 Heisenberg chain," Sov. J. Nucl. **32**, 298–303.